Published in final edited form as:

J Am Chem Soc. 2019 February 20; 141(7): 3083–3099. doi:10.1021/jacs.8b12247.

Development of a Terpene Feedstock-based Oxidative Synthetic Approach to the *Illicium* Sesquiterpenes

K Hung[1,§], **ML Condakes**[1,§], **LFT Novaes**[1], **SJ Harwood**[1], **T Morikawa**[1], **Z Yang**[1], and **TJ Maimone**[1,*]

[1] Department of Chemistry, University of California, Berkeley, 826 Latimer Hall, Berkeley, California 94720, United States.

Abstract

The *Illicium* sesquiterpenes are a family of natural products containing over 100 highly oxidized and structurally complex members, many of which display interesting biological activities. This comprehensive account chronicles the evolution of a semisynthetic strategy toward these molecules from (+)-cedrol, seeking to emulate key aspects of their presumed biosynthesis. An initial route generated lower oxidation state analogs, but failed in delivering a crucial hydroxy group in the final step. Insight gathered during these studies, however, ultimately led to a synthesis of the pseudoanisatinoids along with the *allo*-cedrane natural product 11-*O*-debenzoyltashironin. A second-generation strategy was then developed to access the more highly oxidized majucinoid compounds including jiadifenolide and majucin itself. Overall, one dozen natural products can be accessed from an abundant and inexpensive terpene feedstock. A multitude of general observations regarding site-selective C(sp^3)–H bond functionalization reactions in complex polycyclic architectures are reported.

Graphical Abstract

[*] **Corresponding Author** maimone@berkeley.edu.
[§] **Author Contributions:** K.H. and M.L.C. contributed equally

The authors declare no competing financial interests.

ASSOCIATED CONTENT
Supporting Information
The Supporting Information is available free of charge on the ACS Publications website at DOI: XXXX.
X-ray crystallographic data for **23** (CIF)
X-ray crystallographic data for **37** (CIF)
X-ray crystallographic data for **43** (CIF)
X-ray crystallographic data for **44** (CIF)
X-ray crystallographic data for **48** (CIF)
X-ray crystallographic data for **53** (CIF)
X-ray crystallographic data for **55** (CIF)
X-ray crystallographic data for **58** (CIF)
X-ray crystallographic data for **60** (CIF)
X-ray crystallographic data for **67** (CIF)
X-ray crystallographic data for **70** (CIF)
X-ray crystallographic data for **92** (CIF)
X-ray crystallographic data for **105** (CIF)
X-ray crystallographic data for **107** (CIF)
Experimental procedures and spectroscopic data (PDF)

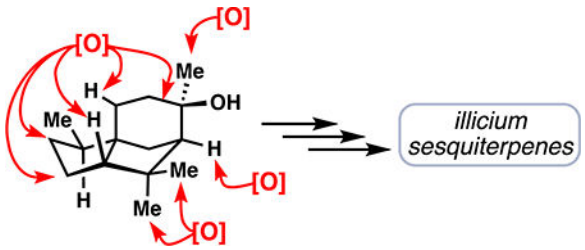

Introduction

To date, over 100 sesquiterpene lactones have been isolated from the *Illicium* genus of plants. Collectively known as the *Illicium* sesquiterpenes, these natural products share a common ring system that is ornately decorated with various oxidation patterns (Figure 1). In fact, every non-quaternary carbon is documented to be oxidized in at least one member of this family. Furthermore, the diversity of oxidations around this common core correlates with the diversity of biological modalities of these molecules.[1]

Initially, isolation of theses natural products was guided by their potent neurotoxic activities. For example, anisatin (**6**), characterized in 1968 by Yamada from Japanese star anise (*Illicium anisatum*), is a convulsant and one of the most potent poisons of plant origin (murine LD_{50} < 1 mg/kg).[2,3] Further studies determined that anisatin, like picrotoxinin, is a strong non-competitive antagonist of the γ-aminobutyric acid receptor ($GABA_AR$).[4] Pseudoanisatin (**5**) was likewise shown to be a $GABA_AR$ antagonist, but it demonstrated remarkable selectivity for insect $GABA_AR$ (IC_{50}^{fly} = 376 nM) over a mammalian $GABA_AR$ ($IC_{50}^{rat} > 10^4$ nM), suggesting utility as an insecticide and highlighting how subtle oxidation state changes in this family lead to profoundly different outcomes.[5]

More recently, however, Fukuyama has shown that other members of this family, including compounds **1**-**4**, do not share this toxicity profile. Many of these compounds promote instead what has been termed a “neurotrophic” phenotype.[6] That is, these compounds have been shown to stimulate neurite outgrowth in cultured rat cortical neurons. For **2**, this observation has also been extended to human induced pluripotent stem cells.[7] Such results have implications in the study of neurodegenerative diseases, such as Alzheimer’s or Parkinson’s.[8] The ostensibly antithetical biological effects of *Illicium* natural products have not gone unnoticed.

Recent investigations by Shenvi and researchers from Eli Lilly demonstrated that these beneficial responses could likewise be traced back to a mechanistically distinct modulation of $GABA_AR$’s.[9]

Against this backdrop of structural intricacies and fascinating biological activities, over 30 inspired syntheses of these molecules have been disclosed.[10] Multiple groups, spanning decades of synthetic investigations, have reported total and formal syntheses of jiadifenolide (**2**),[11] jiadifenin (**3**),[12] 11-*O*-debenzoyl tashironin (**4**),[13] anisatin (**6**),[14] and other members.[15–19] Efficiencies of these routes have varied – from upwards of 40 steps to **6**[14a,b] down to

an impressive 8 steps to **2**[11d] – according to the particular structural subtype, the targeted oxidation pattern, and the synthetic strategy employed.

Given the importance of oxidation pattern not only to the biological activities of these compounds but also to the viability of a given synthetic route, we sought a versatile strategy that would allow us precise but flexible control over the introduction of each oxidation. This full report follows the development of such a strategy–which is unique among all reported synthetic strategies to *Illicium* sesquiterpenes–from its initial conception to a now mature approach that has led to pathways capable of accessing at least a dozen family members.[18,19]

Results and Discussion

Synthetic Planning

Inspired by nature's ability to perform site-selective oxidations on hydrocarbon skeletons, we drew on the proposed biosynthesis of these natural products as a conceptual framework for our own abiotic synthetic work (Figure 2).[1] In essence, cyclizations and hydride shifts from farnesyl pyrophosphate rapidly forge the polycyclic cedrane skeleton (**8**) presumably traversing the ubiquitous bisabolyl cation (**7**). A C–C bond shift event reorganizes this intermediate to the key *allo*- cedrane core (**9**). Direct oxidation of **9** can lead to natural products like **4**, however, if further C–C bond cleavage events take place the *seco*-prezizaane (**10**) and anislactone-type (**12**) skeletons can also be accessed. These proposed ring systems are then tailored to the observed sesquiterpenes by selective enzymatic oxidations.

To recapitulate that biosynthetic endgame, we ideally would have begun our synthesis with a commercially available terpene containing the *seco*-prezizaane carbon skeleton.[20] Indeed, such semisynthetic logic has been employed successfully and extensively in the field of steroid synthesis.[21] Unfortunately, as is the case with most terpenes outside the realm of steroids, we found no starting material fitting those exact criteria; instead, we honed in on (+)-cedrol (**15**), which contains the cedrane skeleton (**8**), as an inexpensive (~$0.05 USD/g), renewable terpene feedstock isolated from Texas cedarwood (Figure 3A).

However, in addition to 6–12 net oxidations needed to convert unfunctionalized **15** to various *Illicium* sesquiterpenes, C–C bond shift and C–C bond cleavage operations would also now have to be incorporated into the synthesis. At this point, we made another observation crucial to our synthetic planning: oxidations at a total of 6 sites (5 C–H bonds and one C–C bond) in **15** were conserved throughout this family. Thus, targeted oxidations of these sites would be a prerequisite to any successful route starting from the cedrane framework.

Many creative approaches towards functionalizing cedrol already have been disclosed in the literature (Figure 3B). Extensive biological studies have been performed using microbes,[22] fungi,[23] rabbits,[24] and dogs[25] to map sites of enzymatic oxidations. Additionally, many chemical methods[26] have been disclosed to modify **15** with varying degrees of efficiency and selectivity. Despite this breadth of literature, modification of only two positions have proven to be amenable to preparative scales – oxidation of the C1 methine[27] and directed

oxidation of the C14 methyl group[28] – underscoring the necessity for novel C(sp^3)–H oxidation methodologies to target other types of strategic bonds.[29,30]

Biomimetic C–C Bond Shift

Originally, we looked to the biosynthesis of these compounds as a direct blueprint for our synthetic efforts. That is, we desired to perform a C–C bond migration to convert the cedrane bicyclo[3.2.1]octane ring system to the *allo*-cedrane bicyclo[2.2.2]octane framework, followed by an intended cleavage of the C6–C11 single bond. While there was similar precedent in the literature for such a ring system conversion (Figure 3C),[31] in which *allo*-cedrane structure **18** was directly accessed from cedrene (**16**) via carbocation **17**, we desired a more highly oxidized substrate for our studies (Scheme 1).

To begin, cedrol (**15**) was dehydrated to cedrene ($CuSO_4$) and then oxidized regioselectively at the C10 position (PIDA, TBHP) affording cedrenone (**19**).[32, 33] Further allylic oxidation (SeO_2 followed by $NaClO_2$) afforded carboxylic acid **20** rapidly, with strategically positioned functionality for further transformations. Epoxidation of **20** (H_2O_2, NaOH), while proceeding only to low conversion nevertheless gave ring shift substrate **21** in useful quantities for exploratory studies.[34]

At this point, we envisioned that the ring shift could proceed biomimetically through an acid-catalyzed epoxide opening cascade. Cognizant that forming a carbocation would be challenging on such an electron-poor system, we explored strong Lewis acids at elevated temperatures to effect this transformation.[35] Titanium(IV) chloride was determined to be a competent mediator for this reaction, yielding **23** as the only isolated ring-shift product. Notably, the carbocation remaining after the C–C bond shift was quenched by chloride present from the Lewis acid. X-ray analysis allowed us to confirm the connectivity and stereochemistry of **23**, thus validating our proposed biomimetic transformation.

With a proof-of-concept ring shift in hand, we turned our attention to the next biomimetic step: C–C bond cleavage. Although it seemed reasonable that **23** was well suited for retro-aldol type reactivity to break the C6–C11 bond and eliminate chloride, we were unable to determine conditions for such a transformation. Coupled with concerns over material throughput and an inability to improve the yield of **23**, this roadblock impelled us to re-evaluate our synthetic strategy. Rather than beginning with the ring shift, we reasoned, what if instead we switched the order of skeletal transformations and cleaved the C6–C11 bond first? Stepping outside the confines of strict biomimetic logic led us to our next generation synthetic strategy and ultimately to successful abiotic syntheses of these natural products.

Synthesis of the *Seco*-prezizaane Core by a Key Oxidation of C7

Instead of pursuing a C–C single bond cleavage reaction again, we considered it more straightforward to cleave the C6–C11 double bond formed after dehydration of **15** (Figure 4A). Such an approach had the added benefit of installing many requisite oxidations in a single operation. Fortunately, known conditions for the oxidative cleavage of cedrene ($RuCl_3$/$NaIO_4$) proved readily scalable thus delivering **24** and allowing us to focus next on a novel ring shift reaction.[27b]

Noting that each natural product contains oxidation at C7 inspired us to pursue an α-ketol rearrangement to transform the 5,5-cedrane ring system to the 5,6-*seco*-prezizaane one.[36] Moreover, a hydroxyl group at C7 was expected to facilitate C–C bond migration relative to systems like **21**. We quickly determined, however, that standard enolate oxidation reactions were unsuccessful at providing serviceable amounts of C7 oxidized products. Examining conditions in the literature, we came across a few isolated reports of copper(II) salts (which typically perform ketone α-halogenation reactions) mediating direct carbonyl α-oxidations with oxygen nucleophiles.[37] Fortunately, conditions employing $CuBr_2$ translated well to our system, giving lactone **25** in good yield. Interestingly, ketone **25** was not further brominated in this reaction.

The key ring shift was finally brought about from **25** by lactone saponification with concomitant anionic α-ketol rearrangement (KOH, KO*t*-Bu), yielding **26** as a thermodynamic 5.5:1 mixture of diastereomers at C6.[38,39] Having rearranged the cedrane skeleton successfully with multiple oxidations installed in the process, we were poised to address a lynchpin transformation in the synthesis: the C4 methine oxidation.

Before moving ahead with that reaction, though, we were interested in further studying the copper(II) bromide-mediated C7 oxidation to better understand its synthetic utility.

$CuBr_2$-Mediated Oxidative Lactonization

First, we wondered whether this transformation could be extended to substrates with less preorganization. We quickly determined that aromatic keto-acids worked exceptionally well under these conditions, with **27** and **28** being formed in high yield (Figure 4B). The reaction efficiency was not impacted by the introduction of electron-donating (see **29**) or electron-withdrawing (see **30**) groups, and these conditions were compatible with benzylic C–H bonds (see **31**) as well. Increasing the steric bulk proximal to the reaction site as in **32** did not negatively impact the transformation either. Finally, even a simple heteroaromatic structure (see **33**) led to the desired product, albeit in a slightly depressed yield. These transformations are notable for their high yields and operational simplicity (no aqueous workup is required).

Extending this chemistry to complex aliphatic substrates led to interesting results that informed our understanding of the reaction (Figures 4C and 4D). Substrate **34** was prepared in four steps from oleanic acid and, when subjected to our conditions, led to small amounts of expected product **36** (<10% yield). The major product (72% yield) of the reaction was characterized as rearranged lactone **37** and its structure was confirmed by X-ray crystallographic analysis. To rationalize the formation of these products, we infer the intermediacy of a cation adjacent to the ketone (see **35** or related radical cation) which is consistent with direct oxidation of an enol precursorby Cu(II).[40] Attack of the pendent carboxylate onto this carbocation leads to **36** (see "*path a*," in blue), while Wagner-Meerwein shift of the adjacent methyl group prior to carboxylate attack (see "*path b*," in green) explains the presence of **37**.[41]

Additionally, cyclopropane-containing substrate **38** (prepared in one step from (+)-3-carene) was designed to further probe potential radical cation intermediates. Remarkably,

extensively oxidized products **41** and **42** were isolated as the major products of the reaction wherein cyclopropane ring opening was observed.[42] The initial product formed, presumably lactone **40**, then underwent further oxidation to butenolide **42**. An additional ketone α-bromination reaction, as is typical of this reagent, ultimately formed **41**. The reactions of **34** and **38** suggest that further examination of this simple reagent for inducing direct oxidative rearrangements in complex settings is warranted.

C4 Methine Oxidation

With a simple and scalable route to bicycle **26**, we proceeded to address oxidation of the C4 methine position (Figure 5). Buried in the interior of the ring system, the C4 methine position is oxidized reliably in all *Illicium* sesquiterpene family members. Chemical methods, however, come up against challenging realities when attempting to mimic this process abiotically. First, the C4 position is flanked by two all carbon-quaternary centers. Additionally, the presence of a second methine unit at C1 and of various other oxidizable positions (*e.g.*, C8 methylene and the α-ketol motif itself) further complicate reaction development.

Initially, we wondered whether we would see any inherent selectivity for the C4 position with an electrophilic metal oxidant (Figure 5A). When **26** was treated with *in situ* generated RuO_4 ($RuCl_3$ and $KBrO_3$), instead of observing oxidation of either methine position, α-diketone **43** was isolated as the major product.[43] Furthermore, subjecting **43** to additional RuO_4, or reacting **26** for prolonged reaction times, afforded anhydride **44**, an exhaustive oxidation product lacking a carbon atom (likely lost in the form of carbon dioxide). Crystal structures of **43** and **44** were obtained to confirm the identity of these unusual, highly oxidized products.

Reasoning that a directed reaction might prove more fruitful, we began investigating methodologies to leverage the free carboxylic acid moiety. Initially, we explored a copper mediated process disclosed by Brown, which was successful at targeting a tertiary C–H bond for oxidation in this manner.[44,45] However, on **26**, such conditions gave the same product (**43**) as the ruthenium case. In an attempt to modulate the reactivity of the α-ketol motif, protection of the tertiary alcohol as a silyl ether (TMSCl, imidazole) gave an additional avenue (see **45**) for experimentation. Exposure of **45** to hypoiodite photolysis conditions ($PhI(OAc)_2$, I_2) led to decarboxylative iodination, with no sign of desired C–H functionalization (see **46**).[46] Attempting analogous conditions on amidated substrates also did not deliver any C4 oxidation.[47] The first breakthrough was achieved when employing the iron-catalyzed, acid-directed conditions of White.[48–50]

Treating **45** with commercially available [Fe(*S,S'*-PDP)$(MeCN)_2$][$(SbF_6)_2$] yielded notable amounts of desired C–H oxidized product **47**. Other ligand systems and terminal oxidants were also surveyed (Figure 5B), and all were capable of promoting the desired C–H bond functionalization, forming **47** with comparable efficiencies.[51–53] However, additional products **48** and **49** were observed only when mep was used as ligand. It is possible that the mep architecture supports a slightly less reactive iron(oxo) species, which prevents the oxidative degradation of sensitive ketol **48**. Combined, we were able to isolate 56% yield of

C–H oxidized products using this system. Additionally, free alcohol **48** could be converted back to silylated **47**, facilitating material throughput for the synthesis. The peculiar product **49** is also of note, as we could reproducibly isolate this triply oxidized material. Occasionally, multiple oxidations are seen in the course of a single reaction of this type.[54] By analogy to mechanisms proposed in those cases, we speculate that **49** arose first from oxidation to form a C3–C4 alkene (**50**). That alkene then underwent further reaction at the C2 position, leading to a product of oxidative lactonization, containing an alkene at C2–C3 and lactone at C4. Finally, the C2–C3 alkene was epoxidized in a non-directed manner by the catalyst. Nevertheless, with **47** successfully formed, we could proceed onward to late-stage explorations.

Late-Stage Observations and Unsuccessful C14 Oxidation

To functionalize the 5-membered ring further and begin to access pseudoanisatin-like compounds, it was deemed necessary to eliminate the fused lactone of **47** (Scheme 2). Lactone **47** was eliminated under the alkylative action of ethyl Meerwein's salt, smoothly producing trisubstituted alkene **51** after desilylation (TBAF). To access the *trans* diol motif seen in **5**, we initially opted for an epoxide opening strategy. Thus, **51** was epoxidized under vanadium catalysis ($VO(acac)_2$, TBHP), delivering **52** in near quantitative yield as a single isomer.

With a pendant carboxylate at C11, **52** seemed primed for an intramolecular opening of the epoxide at the less substituted C3 position. Unfortunately, various basic conditions reliably led to opening of the epoxide at the C4 position (e.g., KOH, EtOH). The regiochemistry of epoxide opening was confirmed by X-ray analysis of **53**, a reduced derivative formed from $Me_4NBH(OAc)_3$.

Given the proclivity of the ester to promote undesirable reactivity, we attempted obviate the issue by forming a lactone: **52** was reduced ($Me_4NBH(OAc)_3$) and then treated with sodium hydride to promote lactonization and forge **54**. However, **54** similarly resisted opening at the C3 position with a range of heteroatom nucleophiles. Furthermore, attempts to open the epoxide by elimination were uniformly unsuccessful. Surprisingly, treating **54** with LDA did not create a C2–C3 alkene; instead, intramolecular displacement of the epoxide by a lactone enolate occurred preferentially at the C4 position, affording **55** in good yield.[55] The remarkable cyclopropanated structure was confirmed by single crystal X-ray analysis.

Moving away from epoxide opening chemistry, we focused instead on a dihydroxylation approach for alkene functionalization. Intriguingly, two closely related substrates, **51** and **57** behaved quite differently under identical dihydroxylation conditions (OsO_4, pyridine). While **51** was dihydroxylated from the β-face exclusively to give **56**, **57** reacted only from the α-face, providing **58** in high yield. Indeed, the rigidifying conformational influence of the C7–C11 lactone proved to be a fairly general effect, even when extended to other substrates and reaction manifolds. Tricycle **58** could be epimerized at the C3 position to form **60** by a two-step oxidation (TPAP, NMO) and reduction (LAH) sequence. Crystal structures of both **58** and **60** were obtained to confirm all stereocenters and connectivity in preparation for the final steps of the synthesis.

C14 Oxidation: Revision of Strategy

To synthesize pseudoanisatin (**5**), or a related compound like debenzoyldunnianin (**61**), oxidation of the conserved C14 position was unavoidable. While ambitious, late-stage C–H functionalization reactions have been employed in synthesis[56] and we deemed **60** well-poised for a directed oxidation from the C3 alcohol unit to the C14 methyl center (see dashed green arrow). To our great dismay, alkoxy radical generating conditions, including hypoiodite photolysis ($PhI(OAc)_2$, I_2), nitrite photolysis, or lead- and mercury-based transformations ($Pb(OAc)_4$ and HgO, respectively) were unsuccessful at accessing any desired C14 oxidation.

Rather, C–C bond cleavage (particularly of C3–C4) predominated due to β-scission of the hydroxyl radical, despite a presumably accommodating geometry for C–H abstraction.[57] Other transition metal-catalyzed methods, including C–H silylation by iridium and ruthenium catalysis,[58] were similarly unsuccessful, potentially due to unfavorable strain in the cyclometallation step.

Faced with this impasse, we opted to revise our synthetic strategy. Given that C14 oxidation is conserved throughout the entire family of natural products, introducing it at an earlier stage would still allow us to access the full array of natural products. Thus, we attempted to install it in the first step of the synthesis (Scheme 3). A survey of the literature revealed that direct C14 oxidation of cedrol had already been reported by multiple groups.[28a,b] In our hands, we were able to avoid the use of stoichiometric toxic reagents and could elicit this transformation on large scales. Alkylation and concomitant elimination of the strained tetrahydrofuran intermediate (not shown) with Meerwein's salt then furnished methyl ether **62**. This material was then advanced in five steps to C4 oxidation precursor **65**, in analogy to the previous conversion of **16** to **26** (Figure 4). However, the extra oxidation found in **62** relative to cedrene (**16**) necessitated careful re-optimization of reaction conditions, during which process a serendipitous discovery was made.

A Fortuitous Redox-Relay Event: Formal Synthesis of 11-*O*-Debenzoyltashironin

In the optimized silylation of **65**, an extended acidic workup was necessary to cleave other undesired sites of silylation that occurred over the course of the reaction. However, prolonged stirring of this workup led to the isolation of a new compound as the major reaction product. This material, afforded as a mixture of diastereomers at C6, was characterized as lactone **67** (Scheme 4). Further exploration allowed us to bypass silylation altogether and convert **64** directly to **67** under acidic conditions.

Mechanistically, we believe this reaction proceeds in an acid-dependent manner wherein an enolization event facilitates the ionization of the C6 tertiary alcohol. The resultant oxyallyl cation (see **66**) then gets quenched on C8 by the pendant acid, giving rise to "redox relay" product **67** wherein C6 oxidation has been formally transferred to C8.[59]

At this point, we realized that, like **67**, 11-*O*-debenzoyl-tashironin (**4**) also lacks oxidation at the C6 position. Conveniently, we imparted utility to this unique rearrangement by completing a formal synthesis of **4**, drawing on knowledge gained from related scaffolds.

The lactone of **67** was reductively cleaved (lithium naphthalenide) to give C4 oxidation precursor **68** as a single diastereomer. Once again, the simple iron(mep) architecture was experimentally found to be the most successful mediator for the oxidation. However, in this case, *tert*-butylhydroperoxide was more efficient at promoting the reaction than hydrogen peroxide. Desired product **69** was isolated from the reaction as the major component, with a portion of the material funneling to **70** as well. Since **70** lacked the requisite C4 oxidation, it was not advanced further. Demethylation of **69** by *in situ* generated TMSI (from TMSCl and NaI) with concomitant epimerization of C6 gave ketal **71** as a single isomer that Shenvi has shown can be converted to both **72** and **4** in 5 additional steps.[9a]

Synthetic Entry into the Pseudoanisatinoids

Given the success of two previous iron-mediated C–H functionalization reactions on this system (**45** to **47** and **68** to **69**), we were optimistic that **65** would also be a suitable substrate for this chemistry (Scheme 5). Unfortunately, initial attempts to oxidize **65** were met with very low yields of desired product, likely due to its more highly oxidized, electron-deficient structure and the presence of various sensitive functional groups.

To overcome these inherent limitations, we reasoned that a more highly active iron catalyst was necessary for this transformation. Many classes of nitrogen-based ligands have been prepared for and studied in non-heme iron oxidation catalysis,[60] but comparably few have been used in the context of complex molecule synthesis. Nevertheless, iron complexes supported by the pinene-derived mepp ligand had been shown by Costas to be highly active in the hydroxylation of simpler systems and this architecture was the only one that provided appreciable quantities of C4 oxidized products.[52]

Overall, the optimized reaction conditions afforded the desired product **73** in serviceable yield for the rest of the synthesis. Additionally, **74** and **75** were isolated, reaffirming fears about the lability of the silyl and methyl ethers. Compound **74**, though, could be carried forward in parallel, providing additional material throughput for the synthesis. From this point, following a similar synthetic endgame as before allowed us to complete our first oxidative *Illicium* synthesis: **73** was taken on to (+)-pseudoanisatin (**5**) in five steps (Scheme 5), which also constituted a formal synthesis of (–)-3-oxopseudoanisatin (**78**).[61]

Along the way, (–)-3-deoxypseudoanisatin (**77**) was also synthesized by a radical hydration reaction of key alkene **76**.[62] Notably the diastereoselectivity of this process was modest. In total, 6–8 oxidations were required to arrive at these compounds and a total of five natural products could be synthesized by this route.

New Synthetic Strategy to Circumvent the Iron-Mediated C4 Oxidation

While a gratifying proof of concept, and the first reported route to these molecules, this synthetic strategy nevertheless had areas for improvement. First, we felt there was still room to implement a more successful C4 oxidation as the yields obtained with iron catalysis were not optimal. Second, we wanted to target multiple *Illicium* subtypes with our chemistry, including the more highly oxidized “majucinoids” – natural products containing the C12–C14 γ-lactone of **1**.

To address the first challenge, we considered moving away from acid-directed C–H functionalization and towards alcohol-directed reactivity instead. Alcohol **81** was prepared quickly from **62** in three steps (Scheme 6). Similar compounds were known in the literature to undergo directed C–H abstraction at the C4 position yet these substrates did not possess oxygenation at C14,[27b,28a] now a region of unease for future synthetic planning. Our concerns were realized when we exposed **81** to Suárez-type radical-generating conditions ($PhI(OAc)_2$, I_2); although desired compound **84** was identified, we isolated **83** as the major reaction product – the result of an apparent 1,6-hydrogen atom transfer (HAT). It is known that 1,5-hydrogen atom transfers (HAT) are generally more facile than other 1,*n*-HATs, primarily due to a lack of entropic penalty in the transition state. At the same time, 1,5-HATs are thought to be at an enthalpic disadvantage when compared with 1,6-HATs.[57b] Therefore, for our system, we rationalized that the rigid geometry minimized entropic differences while having exceptionally weak C14 C–H bonds (likely around 92 kcal/mol) magnified the enthalpic differences as well, leading to the observed preference in radical intermediate **82** for 1,6-HAT. We reasoned, then, that tuning the C–H bond strengths of the C14 position might enable us to modulate the selectivity of this reaction. While C–H bonds adjacent to an ether oxygenare significantly weaker (by *ca*. 5 kcal/mol) than a methine C–H bond, bonds next to an ester oxygen are slightly stronger (by *ca*. 1 kcal/mol), leading us to select an acetate protecting group for the C14 position (Scheme 6, *inset*).[63] Synthesis of acetate-protected **86** followed in a straightforward way from chemistry already developed. Gratifyingly, when **86** was subjected to the reaction conditions, no trace of C14 oxidation was observed and the desired C4 oxidation product **87** was isolated in near-quantitative yield. The incredible efficiency of this transformation permitted the reaction to be run routinely on over decagram scale with commercially available reagents – a vast improvement over the previous iron-catalyzed process.

C12 Oxidation: Toward the Majucinoids

With the C4 oxidation suitably addressed, we turned our attention to accessing the higher oxidation states needed for the majucinoids. In particular, the C12 position – which remained a methyl group in (+)-pseudoanisatin – would need to be exhaustively oxidized to the carboxylic acid level for these natural products (Scheme 7).

Before tackling that issue, though, we needed to again cleave the C6–C11 bond crucial for accessing the *seco*-prezizaane skeleton. However, we no longer had an easily functionalized C–C double bond; in **87**, a single bond now connected C6 and C11. A prior finding from Waegell and co-workers on desacetoxy **87** provided a solution to this problem as they had shown that *in situ* generated RuO_4 could oxidatively cleave this C–C bond leading to a keto lactone.[27,28a] We were pleased to find that this highly electrophilic metal oxidant also smoothly cleaved the corresponding bond in **87**. Somewhat surprisingly, the presence of an electron-withdrawing acetate motif at C14 did not deactivate the proximal C6 position to oxidation. In fact, it had little impact on the course of the transformation, in contrast to previously discussed chemistries. In accordance with Waegell's proposal, we observed initial tertiary C–H hydroxylation at C6 giving rise to intermediate **88** prior to formation of **89**.[27a] Additionally, we identified a small amount of C1 oxidized material in this reaction (see **90**), further implicating the C–H oxidation capabilities of the ruthenium reagent employed.[64]

Key intermediate **89** was now well suited to undergo the oxidations required to access the majucinoids. In perhaps the key oxidation of this work, treating **89** with selenium(IV) oxide effected oxidation at all C–H bonds surrounding the ketone, both at C7 and C12, providing **91** after *in-situ* methylation with dimethylsulfate.[65,66] Furthermore, when molecular sieves were excluded from the reaction, a product oxidized further at C10, **92**, could also be isolated from the reaction mixture. The remarkable structure of this sextuple oxidation product, which contains desirable motifs for the synthesis of jiadifenolide (**2**), was confirmed by X-ray analysis. Unfortunately, we were unable to further bias this process toward the formation of **92**.

For this system, stoichiometric selenium(IV) oxide was uniquely able to effect these oxidations. Other common reagents, including basic permanganate, and catalytic variants of this chemistry[66] were unsuccessful at achieving the same selectivity. Even in the successful reactions, careful choice of conditions, including solvent, was crucial for observing these fully oxidized products. Although non-ideal from a green chemistry perspective, we find it remarkable that in only two steps up to 9 oxidations can be elicited.[67]

Synthesis of Majucin and Related Majucinoids

Taken together, these two steps formed the backbone of our entry to the majucinoids (Scheme 8). A combined 7 oxidations were achieved in rapid fashion, positioning **91** advantageously for further manipulations. In order to access a suitable ring-shift substrate, a concessionary reduction was performed (L-selectride) and basic workup of that reaction then triggered a cascade acetate cleavage/lactonization/isomerization sequence (see **93**, **94**), producing **95** exclusively as the enol tautomer. A sequence of oxidation (DMDO), hydrogen bond-assisted thermal α-ketol rearrangement, and directed reduction ($Me_4NBH(OAc)_3$) furnished *trans*-diol **97**, a known precursor to **2**.[11d] Notably, both acidic and basic conditions known to effect α-ketol rearrangements destroyed this sensitive intermediate. Treatment of **97** with *p*-toluenesulfonic acid under carefully controlled conditions forged **98**, a known intermediate in the synthesis of (1*R*,10*S*)-2-oxo-3,4-dehydroxyneomajucin (ODNM, not shown) and **3**.[12c] The transformation of **97** to **98** is significant since it provided a key link between propellane-type lactone systems found in **2** and the δ-valerolactone unit common to majucinoids. Key building block **98** could then be advanced to 2,3-dehydroneomajucin (DHNM, **99**) via enolate oxidation (MoOPh) and one-pot stereochemical adjustment of the secondary hydroxyl group using Hartwig's transfer hydrogenation protocol.[68] Much like key lactone **76** in our pseudoanisatinoid sequence (Scheme 5), **99** could be formally hydrated ($Mn(dpm)_3/PhSiH_3/O_2$) to give neomajucin (**100**) or dihydroxylated (OsO_4/TMEDA)[69] to produce majucin (**1**). Further intramolecular displacement of mesylate **101** also converted **1** into the neurotrophic natural product jiadifenoxolane A (**102**). Overall, this route demonstrated the maturation of our oxidative strategy by providing syntheses of 7 natural products, each requiring at least 10 oxidations from cedrol.

Looking Ahead: Preliminary Studies on C13 Oxidation Toward Anisatinoid Synthesis

With successful syntheses of two *seco*-prezizaane sesquiterpene subtypes – pseudoanisatinoids and majucinoids – our focus naturally turned to the synthesis of the final subtype, the anisatinoids, exemplified by anisatin (**6**) itself. These compounds contain a

unique *spiro*-β-lactone motif connecting the C13 and C14 positions, with the C13 position exhaustively oxidized to the carboxylic acid oxidation level. Notably, C13 is one of the very few positions on the cedrane skeleton that has resisted both enzymatic and chemical oxidations; likewise, we had not come across a means of oxidizing it over the course of our studies Nevertheless, we envisioned leveraging alcohol-directed C–H activation methodologies from C14 in order to oxidize this challenging position. We selected alcohol **103**, prepared in one step from acetate **87**, as a suitable directing group for our initial explorations (Scheme 9). Thus, in one instance, following reactivity disclosed by Hartwig,[58,70] **103** was silylated (Et_2SiH_2) under iridium catalysis, producing silyl ether **104**. Using rhodium catalysis, a dehydrogenative coupling between the silyl center and the C13 position of **104** forged an intermediate oxasilacyclopentane which was directly oxidized under Tamao-Fleming type conditions (H_2O_2) to unveil diol **105**, whose identity was confirmed by X-ray analysis.

In parallel, **103** could be converted to primary sulfamate **106** (NaH, $ClSO_2NH_2$), a substrate set up for nitrenoid C–H insertion chemistry.[71] Chelated rhodium catalyst Rh_2esp_2, with $PhI(OPiv)_2$ as a stoichiometric oxidant, efficiently converted **106** to cyclic sulfamate **107**, whose structure was again confirmed by X-ray analysis.

Notably, both methodologies displayed exquisite regioselectivity for the C13 position, despite the C7 methine being nominally the same distance from the directing group.[72] Such selectivity (particularly from a freely-rotating directing group) for a primary C–H bond over a tertiary one can be challenging to achieve for nitrenoid insertion catalysis.[73] In our case, we believe subtle conformational effects of our rigid system favored this unique reactivity. Importantly, **105** and **107** now have key C–H oxidations in place for preparing the β-lactone motif seen in anisatin (**6**).

Conclusion

In this report, we have detailed the evolution of an oxidative approach to multiple classes of *Illicium* sesquiterpene natural products from (+)-cedrol, work which allows access to one dozen natural products from a renewable terpene feedstock used primarily in fragrance chemistry (Figure 6). Inspired by nature, this strategy further showcased the power of chemical synthesis to perform site-selective C(sp^3)–H bond activations in a designed manner. Despite a wealth of literature reports documenting individual oxidation reactions of cedranes, merging these findings–and incorporating new ones–into a unifying synthetic pathway proved challenging, but rewarding.

An initial route accessed lower oxidation state *Illicium* sesquiterpene analogs, but failed to deliver crucial C14 oxygenation in the final step. However, insight gathered during these studies ultimately led to a synthesis of the pseudoanisatinoids along with the *allo*-cedrane natural product 11-*O*-Debenzoyltashironin. Along the way, many lessons were learned about the strengths, and limitations, of directed and non-directed C–H functionalization in complex settings – particularly for the challenge of C4 and C14 oxidations. The sensitivity of high valent iron-oxo catalysis to small structural changes is of note.

Eventually, we were led to develop a protocol employing a non-heme iron catalyst new to complex molecule synthesis. Moving forward to the synthesis of the majucinoids, we resolved the C4 material throughput dilemma using hypoiodite photolysis conditions instead and discovered a route to rapidly access the increased oxidation states of these molecules leveraging both Waegell's C–C cleavage reaction and a selenium dioxide-mediated quadruple oxidation. Combined with our prior knowledge regarding the ring expansion of *5,5*-fused cedrane skeletons into *5,6*-fused *seco*-prezizaane ones via the α-ketol rearrangement, we completed the first synthesis of majucin and related derivatives

We hope these observations and lessons taken together will provide instructive guidance for future studies in the area of complex molecule synthesis by site-selective C(sp^3)–H oxidation as well as spur the development of improved methodologies for such endeavors.

Supplementary Material

Refer to Web version on PubMed Central for supplementary material.

ACKNOWLEDGMENT

This work is dedicated to Professor E. J. Corey on the occasion of his 90th birthday. Financial support is acknowledged from the NIH (GM116952). T.J.M. acknowledges unrestricted financial support from Novartis, Bristol-Myers Squibb, Amgen, and Eli Lilly. T.J.M. is an Arthur C. Cope Scholar and a Research Corporation Cottrell Scholar. K.H. thanks Eli Lilly for a graduate fellowship. M.L.C. acknowledges UC-Berkeley and the NSF for a Berkeley Graduate Fellowship and NSF Predoctoral Fellowship (DGE-1106400) respectively. L.F.T.N. is grateful to the São Paulo Research Foundation (FAPESP) for a graduate fellowship (2017/18029-6). S.J.H. thanks the UC-Berkeley College of Chemistry for a summer undergraduate research award. The Japanese Society for the Promotion of Science (JSPS) is acknowledged for providing a Research Fellowship for Young Scientists to T.M. We are grateful to Dr. Hasan Celik and Dr. Jeffrey Pelton for NMR spectroscopic assistance and NIH grant GM68933. Dr. Nicholas Settineri and Dr. Antonio DiPasquale are acknowledged for X-ray crystallographic analysis wherein support from NIH Shared Instrument Grant (S10-RR027172) is also acknowledged.

REFERENCES

(1). For a general review, see:Illicium, Pimpinella and Foeniculum; Jodral MM, Ed.; Medicinal and Aromatic Plants – Industrial Profiles; CRC Press: Boca Raton, FL, USA, 2004; Vol. 40.Fukuyama Y; Huang J-M Chemistry and neurotrophic activity of seco-prezizaane- and anislactone-type sesquiterpenes from Illicium species In Bioactive Natural Products (Part L); Studies in Natural Products Chemistry; Atta-ur-Rahman, Ed.; 2005, Vol. 32, p 395.

(2). (a)Lane JF; Koch WT; Leeds NS; Gorin G On the Toxin of Illicium Anisatum. I. The Isolation and Characterization of a Convulsant Principle: Anisatin. J. Am. Chem. Soc 1952, 74, 3211. (b)Yamada K; Takada S; Nakamura S; Hirata Y The Structures of Anisatin and Neoanisatin Toxic Sesquiterpenes from *Illicium anisatum* L. Tetrahedron 1968, 24, 199.

(3). Kouno I; Baba N; Hashimoto M; Kawano N; Takahashi M; Kaneto H; Yang C-S; Sato S Isolation of Three New Sesquiterpene Lactones from the Pericarps of *Illicium majus*. Chem. Pharm. Bull 1989, 37, 2448.

(4). (a)Kudo Y; Oka J-I; Yamada K Anisatin, a potent GABA antagonist, isolated from *Illicium anisatum*. Neuroscience Lett. 1981, 25, 83.(b)Shinozaki H; Ishida M; Kudo Y Effects of anisatin on the GABA action in the crayfish neuromuscular junction. Brain Research 1981, 222, 401. [PubMed: 7284788] (c)Ikeda T; Ozoe Y; Okuyama E; Nagata K; Honda H; Shono T; Narahashi T Anisatin modulation of the gamma-aminobutyric acid receptor-channel in rat dorsal root ganglion neurons. Br. J. Pharmacol 1999, 127, 1567. [PubMed: 10455311]

(5). Kuriyama T; Schmidt TJ; Okuyama E; Ozoe Y Structure–Activity Relationships of *seco*-Prezizaane Terpenoids in γ-Aminobutyric Acid Receptors of Houseflies and Rats. Bioorg. Med. Chem 2002, 10, 1873. [PubMed: 11937345]

(6). (a)Fukuyama Y; Shida N; Kodama M Isodunnianin: A New Sesquiterpene Enhancing Neurite Outgrowth in Primary Culture of Fetal Rat Cerebral Hemisphere from *Illicium tashiroi*. Planta Med. 1993, 59, 181. [PubMed: 8488197] (b)Huang JM; Yokoyama R; Yang CS; Fukuyama Y Merrilactone A, a novel neurotrophic sesquiterpene dilactone from *Illicium merrillianum*. Tetrahedron Lett. 2000, 41, 6111.(c)Huang JM; Yokoyama R; Yang CS; Fukuyama Y Structure and Neurotrophic Activity of *seco*-Prezizaane-Type Sesquiterpenes from *Illicium merrillianum*. J. Nat. Prod 2001, 64, 428. [PubMed: 11325221] (d)Yokoyama R; Huang JM; Yang CS; Fukuyama Y New *seco*-Prezizaane-Type Sesquiterpenes, Jiadifenin with Neurotrophic Activity and 1,2-Dehydroneomajucin from *Illicium jiadifengpi*. J. Nat. Prod 2002, 65, 527. [PubMed: 11975494] (e)Kubo M; Okada C; Huang JM; Harada K; Hioki H; Fukuyama Y Novel Pentacyclic *seco*-Prezizaane-Type Sesquiterpenoids with Neurotrophic Properties from *Illicium jiadifengpi*. Org. Lett 2009, 11, 5190. [PubMed: 19873982] (f)Kubo M; Kobayashi K; Huang J-M; Harada K; Fukuyama Y The first example of *seco*-prezizaane-type norsesquiterpenoids with neurotrophic activity from *Illicium jiadifengpi*. Tetrahedron Lett. 2012, 53, 1231.

(7). Shoji M; Nishioka M; Minato H; Harada K; Kubo M; Fukuyama Y; Kuzuhara T Neurotrophic activity of jiadifenolide on neuronal precursor cells derived from human induced pluripotent stem cells. Biochem. Biophys. Res. Commun 2016, 470, 798. [PubMed: 26809091]

(8). (a)Xu J; Lacoske MH; Theodorakis EA Neurotrophic Natural Products: Chemistry and Biology. Angew. Chem., Int. Ed 2014, 53, 956.(b)Shenvi RA Neurite outgrowth enhancement by jiadifenolide: possible targets. Nat. Prod. Rep 2016, 33, 535. [PubMed: 26891462]

(9). (a)Ohtawa M; Krambis MJ; Cerne R; Schkeryantz JM; Witkin JM; Shenvi RA Synthesis of (–)-11-O-Debenzoyltashironin: Neurotrophic Sesquiterpenes Cause Hyperexcitation. J. Am. Chem. Soc 2017, 139, 9637. [PubMed: 28644021] (b)Witkin JM; Shenvi RA; Li X; Gleason SD; Weiss J; Morrow D; Catow JT; Wakulchik M; Ohtawa M; Lu H-H; Martinez MD; Schkeryantz JM; Carpenter TS; Lightstone FC; Cerne R Pharmacological characterization of the neurotrophic sesquiterpene jiadifenolide reveals a non-convulsant signature and potential for progression in neurodegenerative disease studies. Biochem. Pharmacol 2018, 155, 61. [PubMed: 29940173]

(10). For reviews on the chemical synthesis of Illicium sesquiterpenes, see:Urabe D; Inoue M Total syntheses of sesquiterpenes from *Illicium* species. Tetrahedron 2009, 65, 6271.Condakes ML; Novaes LFT; Maimone TJ Contemporary Synthetic Strategies Toward *Seco*-Prezizaane Sesquiterpenes from *Illicium* Species, J. Org. Chem 2018, 83, 14843. [PubMed: 30525614]

(11). For total and formal syntheses of jiadifenolide, see:Xu J; Trzoss L; Chang WK; Theodorakis EA Enantioselective Total Synthesis of (–)-Jiadifenolide. Angew. Chem. Int. Ed 2011, 50, 3672.Siler DA; Mighion JD; Sorensen EJ An Enantiospecific Synthesis of Jiadifenolide. Angew. Chem. Int. Ed 2014, 53, 5332.Paterson I; Xuan M; Dalby SM Total Synthesis of Jiadifenolide. Angew. Chem. Int. Ed 2014, 53, 7286.Lu HH; Martinez MD; Shenvi RA An eight-step gram-scale synthesis of (–)-jiadifenolide. Nat. Chem 2015, 7, 604. [PubMed: 26100810] Shen Y; Li L; Pan Z; Wang Y; Li J; Wang K; Wang X; Zhang Y; Hu T; Zhang Y Protecting-Group-Free Total Synthesis of (–)-Jiadifenolide: Development of a [4+1] Annulation toward Multisubstituted Tetrahydrofurans. Org. Lett 2015, 17, 5480. [PubMed: 26509873] Gomes J; Daeppen C; Liffert R; Roesslein J; Kaufmann E; Heikinheimo A; Neuburger M; Gademann K Formal Total Synthesis of (–)-Jiadifenolide and Synthetic Studies toward seco-Prezizaane-Type Sesquiterpenes. J. Org. Chem 2016, 81, 11017. [PubMed: 27740748]

(12). For total and formal syntheses of jiadifenin and (1R,10S)-2-oxo-3,4-dehydroxyneomajucin (ODNM), see:Cho YS; Carcache DA; Tian Y; Li Y-M; Danishefsky SJ Total Synthesis of (±)-Jiadifenin, a Non-peptidyl Neurotrophic Modulator. J. Am. Chem. Soc 2004, 126, 14358. [PubMed: 15521747] Carcache DA; Cho YS; Hua Z; Tian Y; Li Y-M; Danishefsky SJ Total Synthesis of (±)–Jiadifenin and Studies Directed to Understanding its SAR: Probing Mechanistic and Stereochemical Issues in Palladium-Mediated Allylation of Enolate-Like Structures J. Am. Chem. Soc 2006, 128, 1016. [PubMed: 16417394] Trzoss L; Xu J; Lacoske MH; Mobley WC; Theodorakis EA Enantioselective Synthesis of (–)-Jiadifenin, a Potent Neurotrophic Modulator Org. Lett 2011, 13, 4554. [PubMed: 21812392] Yang Y; Fu X; Chen J; Zhai H Total Synthesis of (–)-Jiadifnin Angew. Chem., Int. Ed 2012, 51, 9825.Trzoss L; Xu J; Lacoske MH; Mobley WC; Theodorakis EA *Illicium* Sesquiterpenes: Divergent Synthetic Strategy and Neurotrophic Activity Studies. Chem. - Eur. J 2013, 19, 6398. [PubMed: 23526661] Harada K; Imai A; Uto K; Carter RG; Kubo M; Hioki H; Fukuyama Y Synthesis of jiadifenin using Mizoroki-Heck and Tsuji-

Trost reactions. Tetrahedron 2015, 71, 2199.Cheng X; Micalizio GC Synthesis of Neurotrophic *Seco*-prezizaane Sesquiterpenes (1R,10S)-2-Oxo-3,4-dehydroneomajucin, (2S)-Hydroxy-3,4-dehydroneomajucin, and (−)-Jiadifenin. J. Am. Chem. Soc 2016, 138, 1150. [PubMed: 26785051]

(13). For total and formal syntheses of 11-O-debenzoyltashironin, see:Cook SP; Polara A; Danishefsky SJ The Total Synthesis of (±)-11-O-Debenzoyltashironin. J. Am. Chem. Soc 2006, 128, 16440. [PubMed: 17177359] Polara A; Cook SP; Danishefsky SJ Multiple chirality transfers in the enantioselective synthesis of 11-*O*-debenzoyltashironin. Chiroptical analysis of the key cascade. Tetrahedron Lett. 2008, 49, 5906. [PubMed: 19812682] Mehta G; Maity P A total synthesis of 11-*O*-methyldebenzoyltashironin. Tetrahedron Lett. 2011, 52, 1749.Mehta G; Maity P Explorations *en route* to synthesis of tashironins: singlet oxygen cycloaddition to 1,3-cyclopentadienes embedded within *allo*-cedrane framework. Tetrahedron Lett. 2011, 52, 5161.

(14). For total and formal syntheses of anisatin, see:Niwa H; Nisiwaki M; Tsukada I; Ishigaki T; Ito S; Wakamatsu K; Mori T; Ikagawa M; Yamada K Stereocontrolled Total Synthesis of (–)-Anisatin: A Neurotoxic Sesquiterpenoid Possessing a Novel Spiro β-Lactone. J. Am. Chem. Soc 1990, 112, 9001.Ogura A; Yamada K; Yokoshima S; Fukuyama T Total Synthesis of (–)-Anisatin. Org. Lett 2012, 14, 1632. [PubMed: 22369157] For synthetic studies towards anisatin, including a synthesis of 10-deoxyanisatin (modern numbering) by Kende, see:Lindner DL; Doherty JB; Shoham G; Woodward RB Intramolecular ene reaction of glyoxylate esters: an anisatin model study. Tetrahedron Lett. 1982, 23, 5111.Kende AS; Chen J Stereoselective Total Synthesis of (±)-8-Deoxyanisatin. J. Am. Chem. Soc 1985, 107, 7184.Niwa H; Mori T; Hasegawa T; Yamada K Stereocontrolled Synthesis of Polyfunctionalized *trans*-Hydrindan Systems: A Model Study toward Anisatin. J. Org. Chem 1986, 51, 1015.Loh T-P; Hu Q-Y Synthetic Studies toward Anisatin: A Formal Synthesis of (±)-8-Deoxyanisatin. Org. Lett 2001, 3, 279. [PubMed: 11430054]

(15). For total and formal syntheses of merrilactone A, along with synthetic studies, see:Birman V; Danishefsky SJ The Total Synthesis of (±)-Merrilactone A. J. Am. Chem. Soc 2002, 124, 2080. [PubMed: 11878938] Inoue M; Sato T; Hirama M Total Synthesis of Merrilactone A. J. Am. Chem. Soc 2003, 125, 10772. [PubMed: 12952441] Iriondo-Alberdi J; Perea-Buceta JE; Greaney MF A Paternò-Büchi Approach to the Synthesis of Merrilactone A. Org. Lett 2005, 7, 3969. [PubMed: 16119944] Harada K; Kato H; Fukuyama Y Synthetic studies toward merrilactone A: a short synthesis of AB ring motif. Tetrahedron Lett. 2005, 46, 7407.Meng Z; Danishefsky SJ A synthetic pathway to either enantiomer of merrilactone A. Angew. Chem. Int. Ed 2005, 44, 1511.Mehta G; Singh SR Total Synthesis of (±)-Merrilactone A. Angew. Chem. Int. Ed 2006, 45, 953.Inoue M; Sato T; Hirama M Asymmetric total synthesis of (–)-merrilactone A: use of a bulky protecting group as a long-range stereocontrolling element. Angew. Chem. Int. Ed 2006, 45, 4843.Inoue M; Lee N; Kasuya S; Sato T; Hirama M; Moriyama M; Fukuyama Y Total Synthesis and Bioactivity of an Unnatural Enantiomer of Merrilactone A: Development of an Enantioselective Desymmetrization Strategy. J. Org. Chem 2007, 72, 3065. [PubMed: 17355151] He W; Huang J; Sun X; Frontier AJ Total Synthesis of (±)-Merrilactone A via Catalytic Nazarov Cyclizaiton J. Am. Chem. Soc 2007, 129, 498. [PubMed: 17227006] He W; Huang J; Sun X; Frontier AJ Total Synthesis of (±)-Merrilactone A. J. Am. Chem. Soc 2008, 130, 300. [PubMed: 18067294] Shi L; Meyer K; Greaney MF Synthesis of (±)-Merrilactone A and (±)-Anislactone A. Angew. Chem., Int. Ed 2010, 49, 9250.Chen J; Gao P; Yu F; Yang Y; Zhu S; Zhai H Total Synthesis of (±)-Merrilactone A. Angew. Chem. Int. Ed. 2012, 51, 5897.Nazef N; Davies RDM; Greaney MF Formal Synthesis of Merrilactone A Using a Domino Cyanide 1,4-Addition–Aldol Cyclization. Org. Lett 2012, 14, 3720. [PubMed: 22770228] Inoue M; Urabe D Chapter 5 - Symmetry-Driven Total Synthesis of Merrilactone A and Resolvin E2 In Strategies and Tactics in Organic Synthesis; Harmata M, Ed.; Academic Press: London, 2013; Vol. 9, p 149.Liu W; Wang B Synthesis of (±)-Merrilactone A by Desymmetrization Strategy. Chem. Eur. J 2018, 24, 16511. [PubMed: 30144188]

(16). For total and formal syntheses of anislactone A, along with synthetic studies, see:Hong B-C Shr Y-J; Wu J-L; Gupta AK; Lin K-J Novel [6 + 2] Cycloaddition of Fulvenes with Alkenes: A Facile Synthesis of the Anislactone and Hirsutane Framework. Org. Lett 2002, 4, 2249. [PubMed: 12074679] see ref. 15kGreaney MF; Shi L; Nazef N Chapter 4 - Total Synthesis of (±)-Anislactone A and (±)-Merrilactone A In Strategies and Tactics in Organic Synthesis; Harmata M, Ed.; Academic Press: London, 2013; Vol. 9, p 105.

(17). Mehta G; Shinde HM An approach to seco-Prezizaane Sesquiterpenoids: Enantioselective Total Synthesis of (+)-1S-Minwanenone. J. Org. Chem 2012, 77, 8056. [PubMed: 22897237]

(18). Hung K; Condakes ML; Morikawa T; Maimone TJ Oxidative Entry into the Illicium Sesquiterpenes: Enantiospecific Synthesis of (+)-Pseudoanisatin. J. Am. Chem. Soc 2016, 138, 16616. [PubMed: 27966918]

(19). Condakes ML; Hung K; Harwood SJ; Maimone TJ Total Syntheses of (–)-Majucin and (–)-Jiadifenoxolane A, Complex Majucin-Type Illicium Sesquiterpenes. J. Am. Chem. Soc 2017, 139, 17783. [PubMed: 29148748]

(20). Brill ZG; Condakes ML; Ting CP; Maimone TJ Navigating the Chiral Pool in the Total Synthesis of Complex Terpene Natural Products. Chem. Rev 2017, 117, 11753. [PubMed: 28293944]

(21). For selected modern examples (within the past ten years) and reviews, see:Lednicer D Steroid Chemistry at a Glance; Wiley, 2011.Shenvi RA; Guerrero CA; Shi J; Li C-C; Baran PS Synthesis of (+)-Cortistatin A. J. Am. Chem. Soc 2008, 130, 7241. [PubMed: 18479104] Giannis A; Heretsch P; Sarli V; Stößel A Synthesis of Cyclopamine Using a Biomimetic and Diastereoselective Approach. Angew. Chem. Int. Ed 2009, 48, 7911.Fortner KC; Kato D; Tanaka Y; Shair MD Enantioselective Synthesis of (+)-Cephalostatin 1. J. Am. Chem. Soc 2010, 132, 275. [PubMed: 19968285] Gui J; Wang D; Tian W Biomimetic Synthesis of 5,6-dihydro-glaucogenin C: Construction of the Disecopregnane Skeleton by Iron(II)-Promoted Fragmentation of an α-Alkoxy Hydroperoxide. Angew. Chem. Int. Ed 2011, 50, 7093.Jana CK; Hoecker J; Woods TM; Jessen HJ; Neuburger M; Gademann K Synthesis of Withanolide A, Biological Evaluation of Its Neuritogenic Properties, and Studies on Secretase Inhibition. Angew. Chem. Int. Ed 2011, 50, 8407.Renata H; Zhou Q; Baran PS Strategic Redox Relay Enables A Scalable Synthesis of Ouabagenin, A Bioactive Cardenolide. Science 2013, 339, 59. [PubMed: 23288535] See YY; Herrmann AT; Aihara Y; Baran PS Scalable C–H Oxidation with Copper: Synthesis of Polyoxypregnanes. J. Am. Chem. Soc 2015, 137, 13776. [PubMed: 26466196] Heinze RC; Lentz D; Heretsch P Synthesis of Strophasterol A Guided by a Proposed Biosynthesis and Innate Reactivity. Angew. Chem. Int. Ed 2016, 55, 11656.Danielsson J; Sun DX; Chen X-Y; Risinger AL; Mooberry SL; Sorensen EJ A Stereocontrolled Annulation of the Taccalonolide Epoxy Lactone onto the Molecular Framework of *trans*-Androsterone. Org. Lett 2017, 19, 4892. [PubMed: 28849658] Wang Y; Ju W; Tian H; Tian W; Gui J Scalable Synthesis of Cyclocitrinol. J. Am. Chem. Soc 2018, 140, 9413. [PubMed: 30008202]

(22). (a)Wang KC; Ho LY; Cheng YS J. Chin. Biochem. Soc 1972, 1, 53.(b)Abraham W-R; Washausen P; Kieslich K Microbial Hydroxylation of Cedrol and Cedrene. Z. Naturforsch 1987, 42, 414. (c)Lamare V; Fourneron JD; Furstoss R; Ehret C; Corbier B Microbial transformations 9. Biohydroxylation of alpha-cedrene and cedrol. Synthesis of an odoriferous minor component of cedar wood essential oil. Tetrahedron Lett. 1987, 28, 6269.(d)Maatooq G; El-Sharkawy S; Afifi MS; Rosazza JPN Microbial Transformation of Cedrol. J. Nat. Prod 1993, 56, 1039.(e)Miyazawa M; Itsuzaki Y; Ishikawa K; Ishisaka K Stereospecific hydroxylation of (+)-cedrol by using human skin microbial flora Staphylococcus epidermidis. Nat. Prod. Res 2003, 17, 313. [PubMed: 14526908]

(23). (a)Hanson JR; Nasir H Biotransformation of the sesquiterpenoid, cedrol, by Cephalosporium aphidicola. Phytochem. 1993, 33, 835.(b)Gand E; Hanson JR; Nasir H The biotransformation of 8-epicedrol and some relatives by Cephalosporium aphidicola. Phytochem. 1995, 39, 1081. (c)Fraga BM; Guillermo R; Hanson JR; Truneh A Biotransformations of cedrol and related compounds by Mucor plumbeus. Phytochem. 1996, 42, 1583.(d)Collins OD; Reese PB Biotransformation of cedrol by Curvularia lunata ATCC 12017. Phytochem. 2001, 56, 417. (e)McCook KP, Chen ARM; Reynolds WF; Reese PB The potential of Cyathus africanus for transformation of terpene substrates. Phytochem. 2012, 82, 61.(f)Sultan S; Choudhary MI; Khan SN; Fatima U; Atif M; Ali RA; Rahman A.-u.; Fatmi MQ Fungal transformation of cedryl acetate and α-glucosidase inhibition assay, quantum mechanical calculations and molecular docking studies of its metabolites. Eur. J. Med. Chem 2013, 62, 764. [PubMed: 23455027]

(24). Bang L; Ourisson G Hydroxylation of cedrol by rabbits. Tetrahedron Lett. 1975, 16, 1881.

(25). Trifilieff E; Bang L; Ourisson G Hydroxylation du cedrol par le chien. Tetrahedron Lett. 1975, 16, 4307.

(26). (a)Trifilieff E; Bang L; Ourisson G Hydroxylation par l'ozone de l'acetate de cedryle. Hemi-synthese du nor-cedrenol. Tetrahedron Lett. 1977, 18, 2991.(b)Tori M; Matsuda R; Asakawa Y

Hydroxylation of Cedrol by m-Chloroperbenzoic Acid. Synthesis of an Epimer of the Alleged "Senoxydene." Bull. Chem. Soc. Jpn 1985, 58, 2523.(c)Shiao M-J; Lin JL; Kuo Y-H; Shih K-S Oxidation of unactivated carbon atoms of cedrol and cedrol acetate with *m*-chloroperbenzoic acid. Tetrahedron Lett. 1986, 4059.(d)Barton DHR; Beloeil J-C; Billion A; Boivin J; Lallemand J-Y; Lelandais P; Mergui S Functionalisation of saturated hydrocarbons. Part XI. Oxidation of cedrol, β- and γ-eudesmol, sclareol, manoyl oxide, 1,9-dideoxyforskolin, methyl trans-dihydroiasmonate, and tetrahydrolinalool by the 'Gif system.' Helv. Chim. Acta 1987, 70, 2187. (e)Guo J-J; Hu A; Chen Y; Sun J; Tang H; Zuo Z Photocatalytic C−C Bond Cleavage and Amination of Cycloalkanols by Cerium(III) Chloride Complex. Angew. Chem. Int. Ed 2016, 55, 15319.(f)Bunescu A; Butcher TW; Hartwig JF Traceless Silylation of β-C(sp3)–H Bonds of Alcohols via Perfluorinated Acetals. J. Am. Chem. Soc 2018, 140, 1502. [PubMed: 29283571] (g)Carestia AM; Ravelli D; Alexanian EJ Reagent-dictated site selectivity in intermolecular aliphatic C–H functionalizations using nitrogen-centered radicals. Chem. Sci 2018, 9, 5360. [PubMed: 30009007]

(27). (a)Tenaglia A; Terranova E; Waegell B Ruthenium-catalyzed C–H bond activation oxidation of bridged bicyclic and tricyclic alkanes. Tetrahedron Lett. 1989, 30, 5271.(b)Tenaglia A; Terranova E; Waegell B Ruthenium-catalyzed carbon-hydrogen bond activation. Oxyfunctionalization of nonactivated carbon-hydrogen bonds in the cedrane series with ruthenium tetraoxide generated in situ. J. Org. Chem 1992, 57, 5523.(c)Gómez L; Canta M; Font D; Prat I Ribas, X.; Costas, M. Regioselective Oxidation of Nonactivated Alkyl C–H Groups Using Highly Structured Non-Heme Iron Catalysts. J. Org. Chem 2013, 78, 1421. [PubMed: 23301685] (d)Jana S; Ghosh M; Ambule M; Sen Gupta S Iron Complex Catalyzed Selective C–H Bond Oxidation with Broad Substrate Scope. Org. Lett 2017, 19, 746. [PubMed: 28134527] (e)Mack JBC; Gipson JD; Du Bois J; Sigman MS Ruthenium-Catalyzed C–H Hydroxylation in Aqueous Acid Enables Selective Functionalization of Amine Derivatives. J. Am. Chem. Soc 2017, 139, 9503. [PubMed: 28660763] (f)Chandra B; Singh KK; Sen Gupta S Selective photocatalytic hydroxylation and epoxidation reactions by an iron complex using water as the oxygen source. Chem. Sci 2017, 8, 7545. [PubMed: 29163909]

(28). (a)Brun P; Waegell B Heterocyclisation intramoleculaire d'alcools possedant un squelette cedranique. Oxydation par le tetraacetate de plomb et par l'oxyde de mercure et le brome. Tetrahedron 1976, 32, 1137.(b)Dorta RL; Francisco CG; Freire R; Suárez E Intramolecular hydrogen abstraction. The use of organoselenium reagents for the generation of alkoxy radicals. Tetrahedron Lett. 1988, 29, 5429.(c)(d)

(29). For recent reviews on C–H bond functionalization in synthesis, see:Gutekunst WR; Baran PS C–H functionalization logic in total synthesis. Chem. Soc. Rev 2011, 40, 1976. [PubMed: 21298176] Newhouse T; Baran PS If C–H Bonds Could Talk: Selective C–H Bond Oxidation. Angew. Chem., Int. Ed 2011, 50, 3362.Chen DY-K; Youn SW C–H Activation: A Complementary Tool in the Total Synthesis of Complex Natural Products. Chem. - Eur. J 2012, 18, 9452. [PubMed: 22736530] Hartwig JF Evolution of C–H Bond Functionalization from Methane to Methodology. J. Am. Chem. Soc 2016, 138, 2. [PubMed: 26566092] Tao P; Jia Y C–H bond activation in the total syntheses of natural products. Sci. China: Chem 2016, 59, 1109.Qiu Y; Gao S Trends in applying C–H oxidation to the total synthesis of natural products. Nat. Prod. Rep 2016, 33, 562. [PubMed: 26847167] Chen K; Lei X Recent applications of C–H functionalization in complex molecule synthesis. Curr. Opin. Green Sustain. Chem 2018, 11, 9.Abrams DJ; Provencher PA; Sorensen EJ Recent applications of C–H functionalization in complex natural product synthesis, Chem. Soc. Rev 2018, 47, 8925. [PubMed: 30426998]

(30). For an example of unactivated C(sp3)–H functionalization in the context of an Illicium member synthesis, see ref. 11b.

(31). McAndrew BA; Meakins SE; Sell CS; Brown C The acetylation of cedrene in the presence of titanium tetrachloride. J. Chem. Soc., Perkin Trans I 1983, 1373.For related carbocation-based skeletal rearrangements, see:Shanker PS; Rao GSRS Synthesis based on cyclohexadienes. Part 25. Total synthesis of (±)-allo-cedrol (khusiol). J. Chem. Soc. Perkin Trans 1 1998, 539.Sharma MK; Banwell MG; Willis AC Approaches to the Neurotrophically Active Natural Product 11-*O*-Debenzoyltashironin: A Chemoenzymatic Total Synthesis of the Structurally Related Sesquiterpene Khusiol. Asian J. Org. Chem 2014, 3, 632.

(32). Eisenbraun EJ; Payne KW; Bymaster JS Dehydration of cedrol to α-cedrene using copper(II) sulfate and other acidic salts. Org. Prep. Proced. Intl 2000, 32, 557.

(33). Blumann A; Schulz L Über Cedrenen, $C_{15}H_{22}$ und seine Umwandlung in Cedren. Chem. Ber 1931, 1540.

(34). We assume this transformation is difficult due to an unfavorable developing *syn*-pentane interaction between the C12 carboxylate and C14 methyl group in the transition state.

(35). Rajendar G; Corey EJ A Systematic Study of Functionalized Oxiranes as Initiating Groups for Cationic Polycyclization Reactions. J. Am. Chem. Soc 2015, 137, 5837. [PubMed: 25871500]

(36). For reviews, see:Paquette LA; Hofferberth JE The α-Hydroxy Ketone (α-Ketol) and Related Rearrangements. Organic Reactions 2003, 62, 477.Zhang X-M; Tu Y-Q; Zhang F-M; Chen Z-H; Wang S-H Recent applications of the 1,2-carbon atom migration strategy in complex natural product total synthesis. Chem. Soc. Rev 2017, 46, 2272. [PubMed: 28349159]

(37). (a)Numazawa M; Nagaoka M New preparation and controlled alkaline hydrolysis of 21-bromo-20-oxopregnenes. A facile synthesis of deoxycorticoids. J. Org. Chem 2001, 50, 81. (b)Toyota M; Yokota M; Ihara M Remarkable Control of Radical Cyclization Processes of Cyclic Enyne: Total Syntheses of (±)-Methyl Gummiferolate, (±)-Methyl 7β-Hydroxykaurenoate, and (±)-Methyl 7-Oxokaurenoate and Formal Synthesis of (±)-Gibberellin A12 from a Common Synthetic Precursor. J. Am. Chem. Soc 2001, 123, 1856. [PubMed: 11456805] (c)Miyake H; Nishimura A; Yago M; Sasaki M Direct Syntheses of Benzofuran-2(3H)-ones and Benzofuran-3(2H)-ones from 1-(2-Hydroxyphenyl)alkan-1-ones by CuBr2 or CuCl2. Chem. Lett 2007, 36, 332.

(38). Resubjecting the minor isomer to the reaction conditions reestablished this same mixture.

(39). For an example highlighting the reversibility of the α-ketol rearrangement and its interplay with natural product synthesis, see:Wood JL; Stoltz BM; Goodman SN Total Synthesis of (+)-RK-286c, (+)-MLR-52, (+)-Staurosporine, and (+)-K252a. J. Am. Chem. Soc 1996, 118, 10656.

(40). It should be noted that both direct enol oxidation/cation trapping as well as α-bromination/SN2 displacement sequences have been proposed for CuBr2-mediated carbonyl oxyfunctionalizations, see:Glazier ER Bromination with Cupric Bromide. II. Bromination in the Presence of an Olefinic Bond. J. Org. Chem 1962, 27, 4397.

(41). Interestingly, a related DDQ-mediated oxidative lactonization of oleanic acid derivatives does not induce rearrangement, see:Ding Y; Huang Z; Yin J; Lai Y; Zhang S; Zhang Z; Fang L; Peng S; Zhang Y DDQ-promoted dehydrogenation from natural rigid polycyclic acids or flexible alkyl acids to generate lactones by a radical ion mechanism. Chem. Commun 2011, 47, 9495.

(42). Although drawn as a polar cyclopropane ring opening for simplicity, the fragmentation could also plausibly occur through a radical or radical cation intermediate. In this case, oxidation of the resultant tertiary radical to a carbocation would occur prior to lactonization.

(43). This reactivity for RuO4 is relativity uncommon and usually requires strongly acidic media. See, for example:Panda M; Pati SC Ruthenium(VIII) mediated oxidation of some aliphatic and alicyclic ketones by periodate-ruthenium(III) system in aqueous HClO4 medium. Int. J. Chem. Kinet 1996, 28, 453.

(44). (a)Rasik CM; Brown MK Total Synthesis of Gracilioether F: Development and Application of Lewis Acid Promoted Ketene–Alkene [2+2] Cycloadditions and Late-Stage C–H Oxidation. Angew. Chem. Int. Ed 2014, 53, 14522.(b)McCallum ME; Rasik CM; Wood JL; Brown MK Collaborative Total Synthesis: Routes to (±)-Hippolachnin A Enabled by Quadricyclane Cycloaddition and Late-Stage C–H Oxidation. J. Am. Chem. Soc 2016, 138, 2437. [PubMed: 26859526]

(45). Sathyamoorthi S; Du Bois J Copper-Catalyzed Oxidative Cyclization of Carboxylic Acids. Org. Lett 2016, 18, 6308. [PubMed: 27978696]

(46). Concepción JI; Francisco CG; Freire R; Hernández R; Salazar JA; Suárez E Iodosobenzene diacetate, an efficient reagent for the oxidative decarboxylation of carboxylic acids. J. Org. Chem 1986, 51, 402.

(47). (a)Martín A; Pérez-Martín I; Suárez E Intramolecular Hydrogen Abstraction Promoted by Amidyl Radicals. Evidence for Electronic Factors in the Nucleophilic Cyclization of Ambident Amides to Oxocarbenium Ions. Org. Lett 2005, 7, 2027. [PubMed: 15876046] (b)Chen K; Richter JM; Baran PS 1,3-Diol Synthesis via Controlled, Radical-Mediated C−H

Functionalization. J. Am. Chem. Soc 2008, 130, 7247. [PubMed: 18481847] (c)Chen K; Baran PS Total synthesis of eudesmane terpenes by site-selective C–H oxidations. Nature 2008, 459, 824.(d)Richers J; Heilmann M; Drees M; Tiefenbacher K Synthesis of Lactones via C–H Functionalization of Nonactivated C(sp3)–H Bonds. Org. Lett 2016, 18, 6472. [PubMed: 27978701]

(48). (a)Chen M; White MC A predictably selective aliphatic C-H oxidation reaction for complex molecule synthesis. Science 2007, 318, 783. [PubMed: 17975062] (b)Bigi MA; Reed SA; White MC Directed Metal (Oxo) Aliphatic C–H Hydroxylations: Overriding Substrate Bias. J. Am. Chem. Soc 2012, 134, 9721. [PubMed: 22607637]

(49). Iron-catalyzed C–H oxidation reactions have been reviewed, see:Sun C-L; Li B-J; Shi Z-J Direct C–H Transformation via Iron Catalysis. Chem. Rev 2011, 111, 1293. [PubMed: 21049955] White MC; Zhao J Aliphatic C–H Oxidations for Late-Stage Functionalization J. Am. Chem. Soc 2018, 140, 13988. [PubMed: 30185033]

(50). For a recent example of successful iron-catalyzed, acid-directed C–H oxidation in synthesis, see:Ye Q; Qu P; Snyder SA Total Syntheses of Scaparvins B, C, and D Enabled by a Key C–H Functionalization. J. Am. Chem. Soc 2017, 139, 18428. [PubMed: 29227651]

(51). For Fe/mep complexes in C-H oxidation, see:Okuno T; Ito S; Ohba S; Nishida Y μ-Oxo bridged diiron(III) complexes and hydrogen peroxide: oxygenation and catalase-like activities. J. Chem. Soc., Dalton Trans 1997, 3547.Chen K; Que L Jr. Evidence for the participation of a high-valent iron-oxo species in stereospecific alkane hydroxylation by a non-heme iron catalyst. Chem. Commun 1999, 1375.

(52). For Fe/mepp complexes in C–H oxidation, see:Goméz L; Garcia-Bosch I; Company A; Benet-Buchholz J; Polo A; Sala X; Ribas X; Costas M Stereospecific C–H Oxidation with H2O2 Catalyzed by a Chemically Robust Site-Isolated Iron Catalyst. Angew. Chem., Int. Ed 2009, 48, 5720.

(53). For an early use of pyridyl ligand-supported iron complexes in alkane hydroxylation, see:Kim C; Chen K; Kim J; Que L Jr. Stereospecific Alkane Hydroxylation with H2O2 Catalyzed by an Iron(II)–Tris(2-pyridylmethyl)amine Complex. J. Am. Chem. Soc 1997, 119, 5964.

(54). Bigi MA; Reed SA; White CM Diverting non-haem iron catalysed aliphatic C–H hydroxylations towards desaturations. Nature Chem. 2011, 3, 216. [PubMed: 21336327]

(55). Gaoni Y Base induced isomerizations of λ,δ-epoxyketones—II: Syntheses in the thujane series. *d,l*-sabina ketone and *d,l-cis*-sabinene hydrate. Tetrahedron 1972, 28, 5525.Niwa M; Iguchi M; Yamamura S Biogenetic Model Reactions of Epoxygermacrones. Bull. Chem. Soc. Jpn 1976, 49, 3137.For a review of epoxide-opening strategies, see:Salomatina OV; Yarovaya OI; Barkhash VA Intramolecular Involvement of an Oxygen-containing Nucleophilic Group in Epoxy Ring Opening. Russ. J. Org. Chem 2005, 41, 186.

(56). For an assortment of recent C(sp3)–H functionalizations in complex synthesis, see:Quinn RK; Könst ZA; Michalak SE; Schmidt Y; Szklarski AR; Flores AR; Nam S; Horne DA; Vanderwal CD; Alexanian EJ J. Am. Chem. Soc 2016, 138, 696. [PubMed: 26694767] Yuan C; Jin Y; Wilde NC; Baran PS Angew. Chem., Int. Ed 2016, 55, 8280.Kawamura S; Chu H; Felding J; Baran PS Nineteen-step total synthesis of (+)-phorbol. Nature, 2016, 532, 90. [PubMed: 27007853] Kawamata T; Nagatomo M; Inoue MJ Am. Chem. Soc 2017, 139, 1814.Hughes JME; Gleason JL A Concise Enantioselective Total Synthesis of (–)-Virosaine A. Angew. Chem. Int. Ed 2017, 56, 10830.Loskot SA; Romney DK; Arnold FH; Stoltz BM Enantioselective Total Synthesis of Nigelladine A via Late-Stage C–H Oxidation Enabled by an Engineered P450 Enzyme. J. Am. Chem. Soc 2017, 139, 10196. [PubMed: 28721734] Xu L; Wang C; Gao Z; Zhao Y-M Total Synthesis of (±)-Cephanolides B and C via a Palladium-Catalyzed Cascade Cyclization and Late-Stage sp3 C–H Bond Oxidation. J. Am. Chem. Soc 2018, 140, 5653. [PubMed: 29627977] Zhou S; Guo R; Yang P; Li A Total Synthesis of Septedine and 7-Deoxyseptedine J. Am. Chem. Soc 2018, 140, 9025. [PubMed: 29873480] Haines BE; Nelson BM; Grandner JM; Kim J; Houk KN; Movassaghi M; Musaev DG Mechanism of Permanganate-Promoted Dihydroxylation of Complex Diketopiperazines: Critical Roles of Counter-cation and Ion-Pairing. J. Am. Chem. Soc 2018, 140, 13375. [PubMed: 30295476] Zwick CR III; Renata H Remote C−H Hydroxylation by an α−Ketoglutarate-Dependent Dioxygenase Enables Efficient Chemoenzymatic Synthesis of Manzacidin C and Proline Analogs. J. Am. Chem. Soc 2018, 140, 1165. [PubMed: 29283572] Mailyan AK; Chen JL; Li W; Keller AA; Sternisha SM; Miller BG; Zakarian A Short Total

Synthesis of [$^{15}N_5$]−Cylindrospermopsins from $^{15}NH_4Cl$ Enables Precise Quantification of Freshwater Cyanobacterial Contamination. J. Am. Chem. Soc 2018, 140, 6027. [PubMed: 29672038] Dongbang S; Pedersen B; Ellman JA Asymmetric synthesis of (–)-naltrexone. Chem. Sci 2019, 10, 535. [PubMed: 30713650]

(57). It has been proposed that an O•••C distance of 2.5–2.7 Å (or < 3 Å) is necessary for highly-efficient C–H abstractions, seeHeusler K; Kalvoda J Between basic and applied research: Ciba's involvement in steroids in the 1950s and 1960s. Steroids 1996, 61, 492. [PubMed: 8870170] Nechab M; Mondal S; Bertrand MP 1,n-Hydrogen-Atom Transfer (HAT) Reactions in Which n≠5: An Updated Inventory. Chem. Eur. J 2014, 20, 16034. [PubMed: 25345694]

(58). (a)Simmons E;M; Hartwig JF Catalytic functionalization of unactivated primary C–H bonds directed by an alcohol. Nature 2012, 483, 70. [PubMed: 22382981] (b)Li B; Driess M; Hartwig JF Iridium-Catalyzed Regioselective Silylation of Secondary Alkyl C–H Bonds for the Synthesis of 1,3-Diols. J. Am. Chem. Soc 2014, 136, 6586. [PubMed: 24734777] (c)Karmel C; Li B; Hartwig JF Rhodium-Catalyzed Regioselective Silylation of Alkyl C–H Bonds for the Synthesis of 1,4-Diols. J. Am. Chem. Soc 2018, 140, 1460. [PubMed: 29293327] (d)

(59). Isolated instances of similar processes have been reported, see:Jagodziński JJ; Gumułka J; Szczepek WJ Reactions of 5-hydroxy-6-oxo steroids-iii: Acid-catalysed reactions of 3β-acetoxy-5-hydroxy-5α-cholestan-6-one. Tetrahedron 1981, 37, 1015.Morrison GA; Tideswell JA; Wilkinson JB Effect of a Neighbouring Methoxy Group upon the Course of Acid-catalysed Cleavage of a Steroidal Epoxy-ketone. J. Chem. Res. Synop 1990, 7, 222.Elmore SW; Paquette LA A-Ring oxygenation studies in bridgehead hydroxyl-substituted trans-tricyclo[9.3.1.03,8]pentadecan-14-one congeners of taxol. J. Org. Chem 1993, 58, 4963.

(60). Grau M; Britovsek GJP; High-valent iron in biomimetic alkane oxidation catalysis In Iron Catalysis II. Topics in Organometallic Chemistry; Eike Bauer, Ed.; 2015, Vol 50, p 145.

(61). Yokoyama R; Huang J-M; Hosoda A; Kino K; Yang C-S; Fukuyama Y *Seco*-Prezizaane-Type Sesquiterpenes and an Abietane-Type Diterpene from *Illicium minwanense*. J. Nat. Prod 2003, 66, 799. [PubMed: 12828465]

(62). Crossley SWM; Obradors C; Martinez RM; Shenvi RA Mn-, Fe-, and Co-Catalyzed Radical Hydrofunctionalizations of Olefins. Chem. Rev 2016, 116, 8912. [PubMed: 27461578]

(63). (a)Kerr JA; Stoker DW CRC Handbook of Chemistry and Physics in: Lide DR Ed.; CRC Press: Boca Raton, FL, USA 2000;(b)Blanksby SJ; Ellison GB Bond Dissociation Energies of Organic Molecules. Acc. Chem. Res 2003, 36, 255; [PubMed: 12693923] (c)El-Nahas AM; Navarro MV; Simmie JM; Bozzelli JW; Curran HJ; Dooley S; Metcalfe W Enthalpies of Formation, Bond Dissociation Energies and Reaction Paths for the Decomposition of Model Biofuels: Ethyl Propanoate and Methyl Butanoate. J. Phys. Chem. A 2007, 111, 3727. [PubMed: 17286391]

(64). McNeill E; Du Bois J Ruthenium-Catalyzed Hydroxylation of Unactivated Tertiary C−H Bonds. J. Am. Chem. Soc 2010, 132, 10202. [PubMed: 20593904]

(65). An *in-situ* methylation proved necessary to separate the products from various selenium-based and other impurities.

(66). For reviews of selenium-based oxidations, including a discussion of catalytic variants, see:Nicolaou KC; Petasis NA Selenium in Natural Product Synthesis (Philadelphia) 1984Mlochowski J; Wójtowicz-Mlochowska H Developments in Synthetic Application of Selenium(IV) Oxide and Organoselenium Compounds as Oxygen Donors and Oxygen-Transfer Agents Molecules 2015, 20, 10205. [PubMed: 26046320]

(67). For a remarkable selenium dioxide-mediated oxidation in a natural product synthesis, see:Chuang KV; Xu C; Reisman SE A 15-Step Synthesis of (+)-Ryanodol. Science 2016, 353, 912. [PubMed: 27563092]

(68). Hill CK; Hartwig JF Site-selective oxidation, amination and epimerization reactions of complex polyols enabled by transfer hydrogenation. Nature Chem. 2017, 9, 1213. [PubMed: 29168493]

(69). Donohoe TJ; Mitchell L; Waring MJ; Helliwell M; Bell A; Newcombe NJ Homoallylic alcohols and trichloroacetamides as hydrogen bond donors for directed dihydroxylation. Tetrahedron Lett. 2001, 42, 8951.

(70). For a recent example in synthesis, see:Ma X; Kucera R; Goethe OF; Murphy SK; Herzon SB Directed C–H Bond Oxidation of (+)-Pleuromutilin. J. Org. Chem 2018, 83, 6843. [PubMed: 29664634]

(71). (a)Espino CG; Fiori KW; Kim M; Du Bois J Expanding the Scope of C−H Amination through Catalyst Design. J. Am. Chem. Soc 2004, 126, 15378. [PubMed: 15563154] (b)Zalatan DN; Du Bois J Understanding the Differential Performance of Rh2(esp)2 as a Catalyst for C−H Amination. J. Am. Chem. Soc 2009, 131, 7558. [PubMed: 19441831]

(72). Selectivity for the primary position is well-precedented in C(sp3)–H silylation chemistry. For a review on the topic, see:Cheng C; Hartwig JF Catalytic Silylation of Unactivated C–H Bonds. Chem. Rev 2015, 115, 8946. [PubMed: 25714857]

(73). Certain systems are able to effect primary C(sp3)–H amination, for an example see:Paradine SM; Griffin JR; Zhao J; Petronico AL; Miller SM, White MC A manganese catalyst for highly reactive yet chemoselective intramolecular C(sp3)–H amination. Nature Chem. 2015, 7, 987. [PubMed: 26587714]

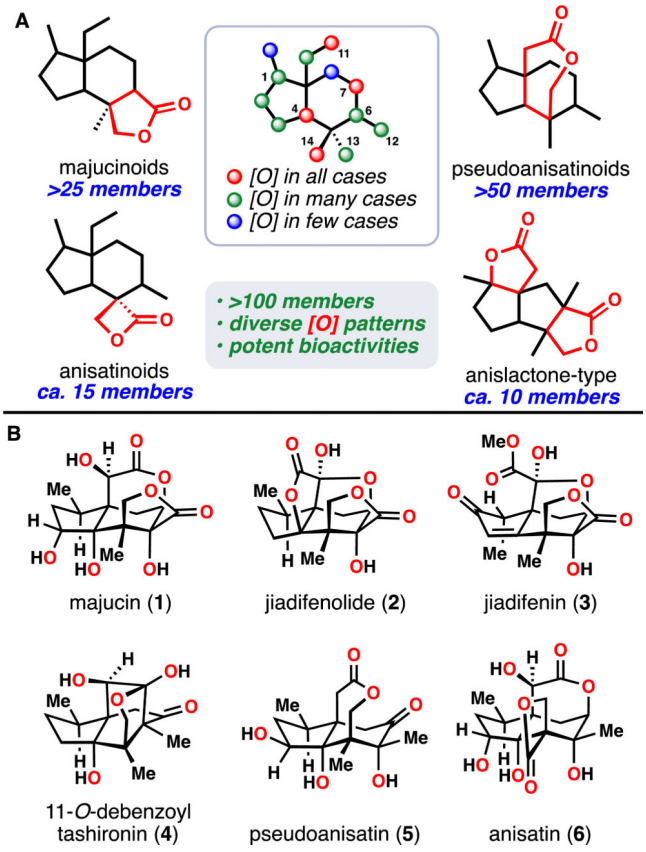

Figure 1.

(A) *Illicium* sesquiterpene family member subtypes characterized by lactonization pattern. Inset: shared skeleton, with an oxidation "heat map" showing the most commonly observed sites of oxidation. **(B)** Representative bioactive *Illicium* sesquiterpenes that have been studied by synthetic chemists.

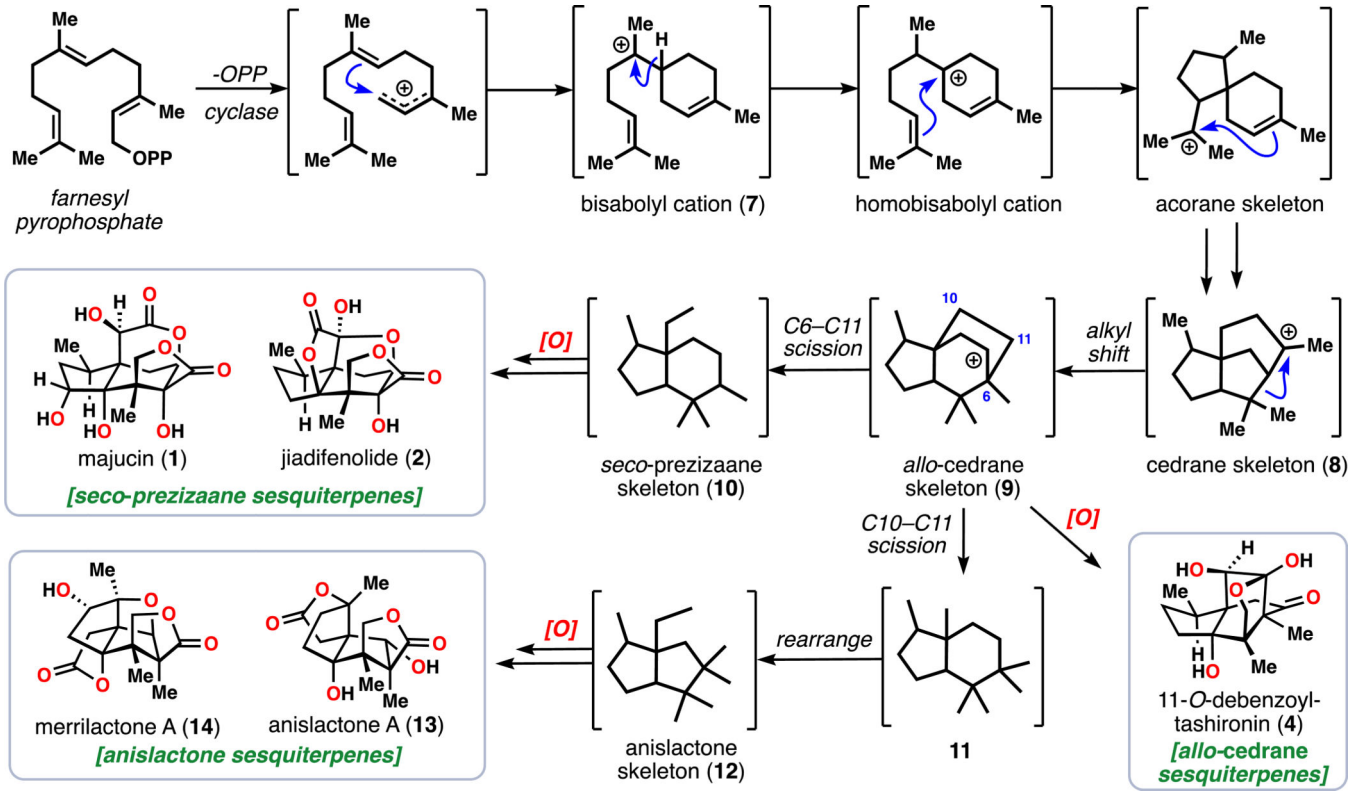

Figure 2.

Fukuyama's proposed biosynthesis of the *Illicium* sesquiterpenes wherein farnesyl pyrophosphate undergoes various cyclizations and rearrangements to reach the core skeletons of the *Illicium* sesquiterpenes, which are then extensively oxidized to arrive at the natural products themselves.

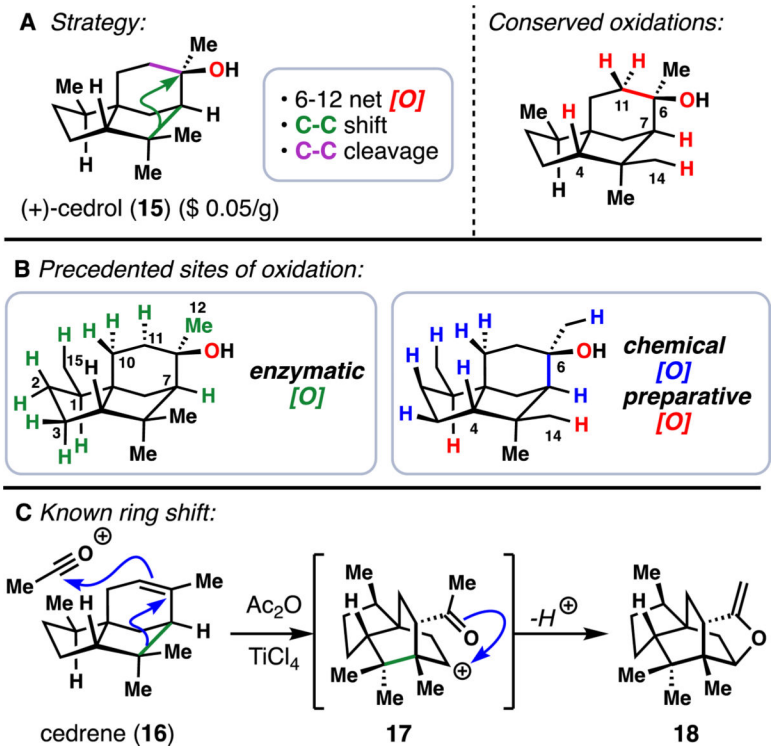

Figure 3.

(A) Overarching synthetic strategy to convert cedrol (**15**) to the *Illicium* sesquiterpenes. **(B)** Known enzymatic (left) and chemical (right) methods for the oxidation of **15**. **(C)** Precedented ring shift to convert the cedrane skeleton to the *allo*-cedrane one.

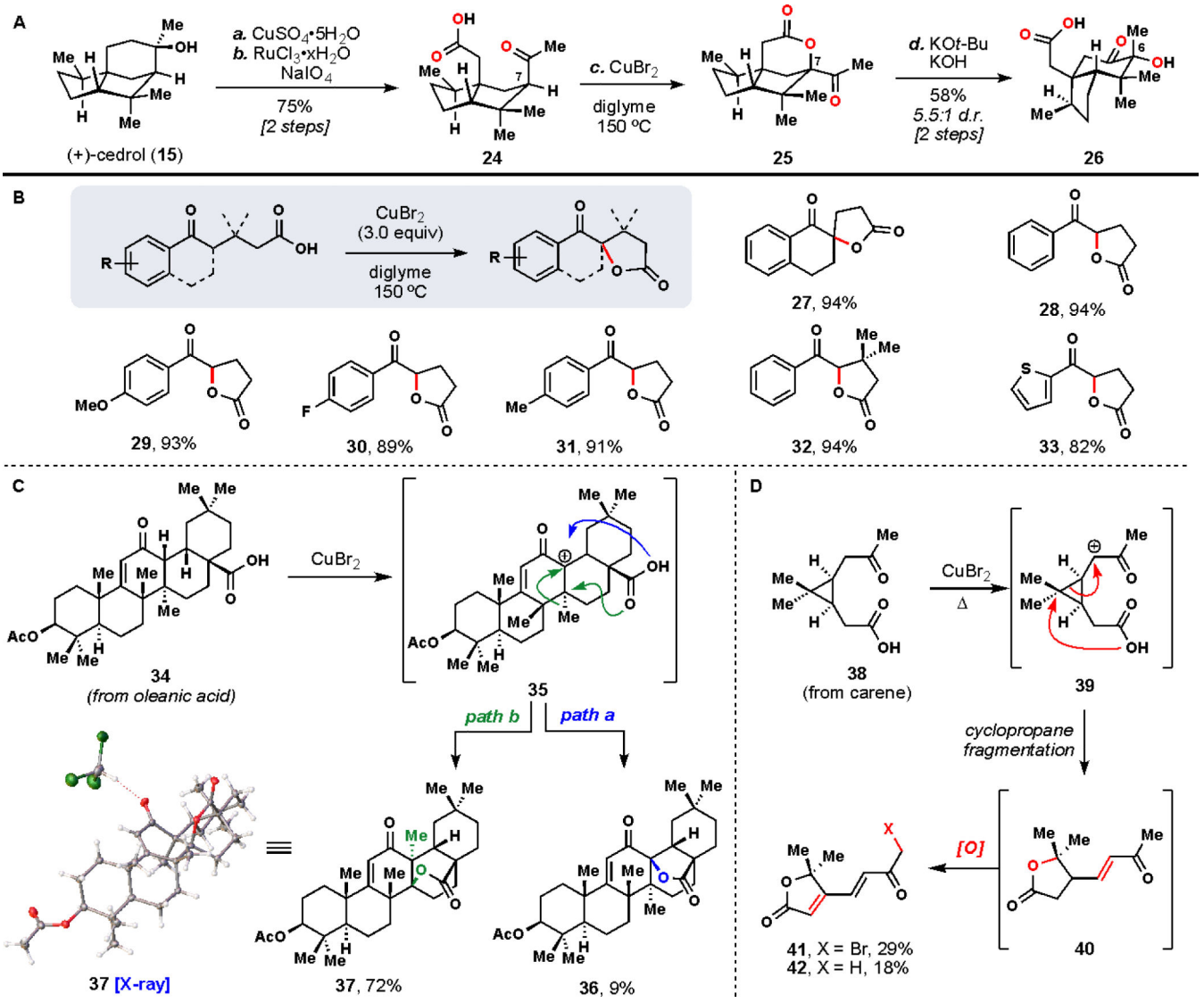

Figure 4.

(A) Successful preparation of the *seco*-prezizaane skeletone from **15** featuring C7 oxidation and an α-ketol rearrangement. **(B)** Extension of the oxidative lactionization reaction to other keto-acid substrates. **(C)** and **(D)** Attempted oxidations of terpene-derived substrates leading to rearranged products.

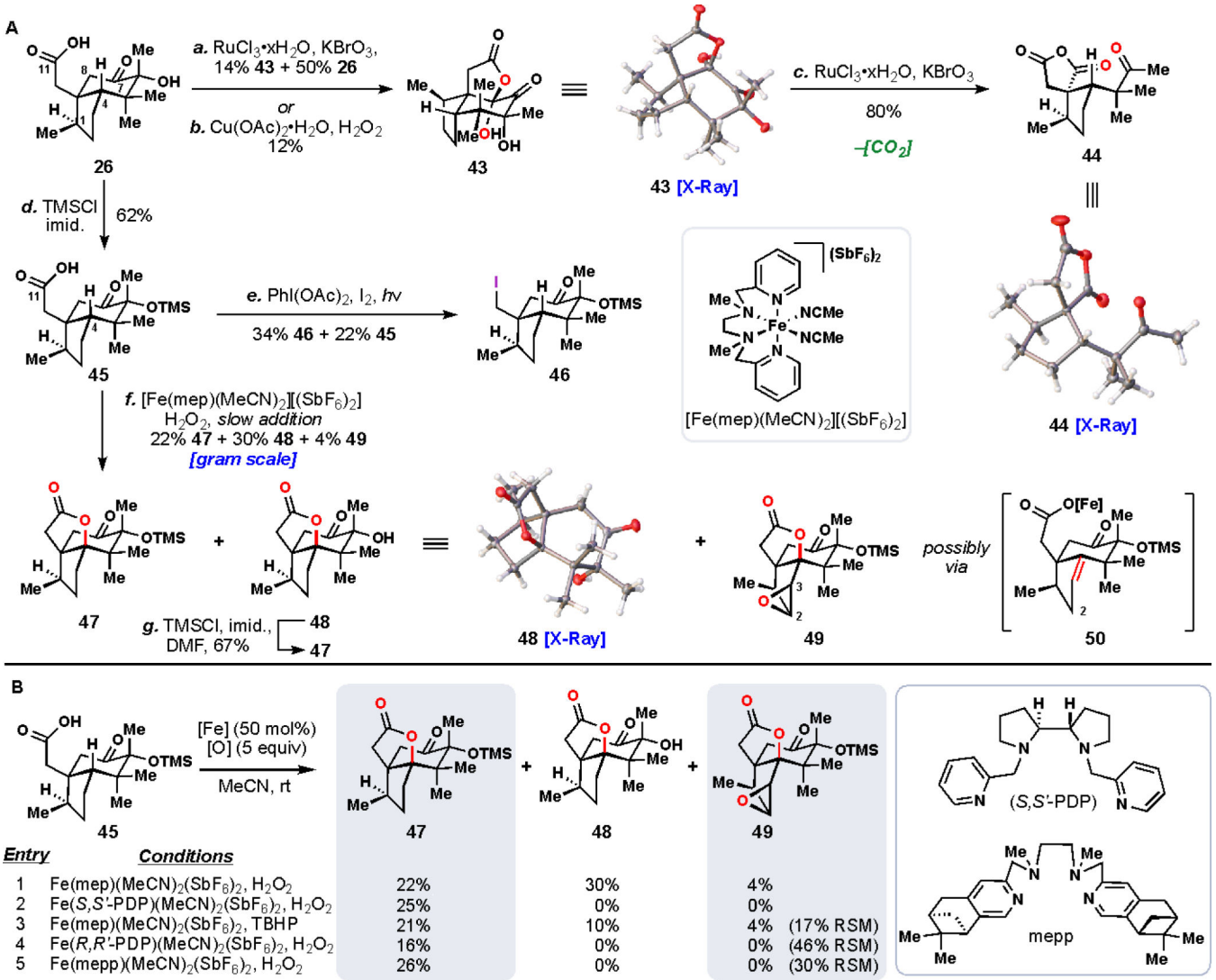

Entry	Conditions	47	48	49	
1	Fe(mep)(MeCN)$_2$(SbF$_6$)$_2$, H$_2$O$_2$	22%	30%	4%	
2	Fe(*S,S'*-PDP)(MeCN)$_2$(SbF$_6$)$_2$, H$_2$O$_2$	25%	0%	0%	
3	Fe(mep)(MeCN)$_2$(SbF$_6$)$_2$, TBHP	21%	10%	4%	(17% RSM)
4	Fe(*R,R'*-PDP)(MeCN)$_2$(SbF$_6$)$_2$, H$_2$O$_2$	16%	0%	0%	(46% RSM)
5	Fe(mepp)(MeCN)$_2$(SbF$_6$)$_2$, H$_2$O$_2$	26%	0%	0%	(30% RSM)

Figure 5.

(A) Synthetic studies towards a successful C4 oxidation **(B)** Optimization of the iron(oxo)-catalyzed C4 oxidation by examination of ligand and terminal oxidant effects

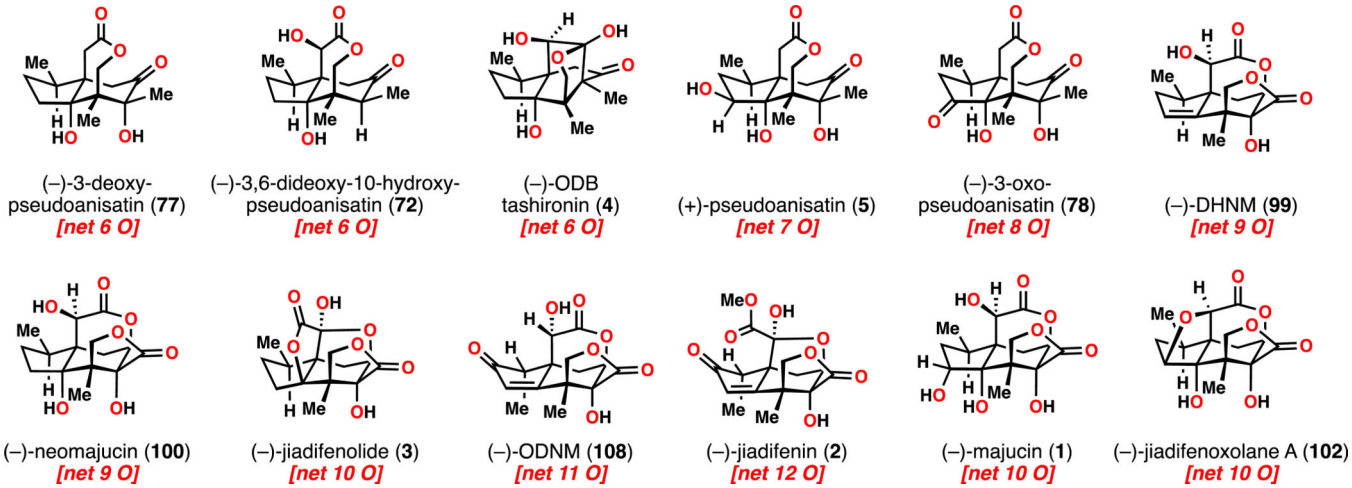

Figure 6.
Current list of *Illicium* sesquiterpene natural products accessible from (+)-cedrol.

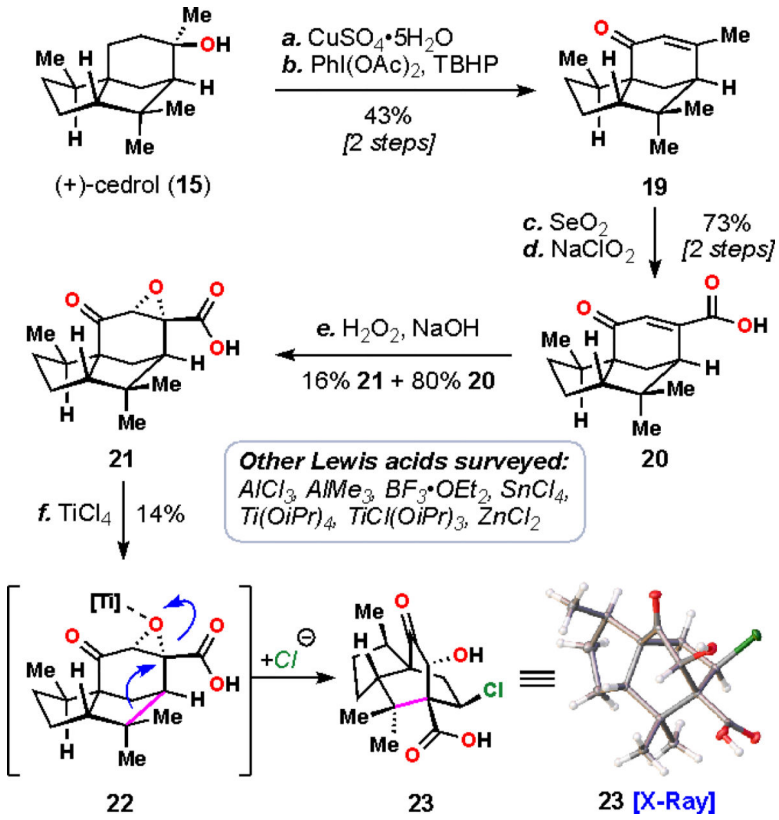

Scheme 1.

Formation of the *Allo*-Cedrane Skeleton[a]

[a]Reagents and conditions: (a) $CuSO_4$•$5H_2O$ (10 mol%), PhH, 80 °C, 4 h; (b) $PhI(OAc)_2$ (3.0 equiv), *tert*-butyl hydroperoxide (70 wt% in H_2O, 4.0 equiv), EtOAc, –20 °C, 12 h, 43% (*two steps*); (c) SeO_2 (2.2 equiv), 1,4-dioxane, 120 °C, 14 h; (d) $NaClO_2$ (10.0 equiv), NaH_2PO_4•H_2O (8.0 equiv), 2-methyl-2-butene (25 equiv), *t*-BuOH:H_2O (1:1), 19 h, 73% (*two steps*); (e) H_2O_2 (50 wt% in H_2O, 10.0 equiv), NaOH (3.0 M, 4.0 equiv), MeOH, 0 → 23 °C, 7 h, 16% (81% BRSM); (f) $TiCl_4$ (1.2 equiv), DCE, 50 °C, 4 h, 14%.

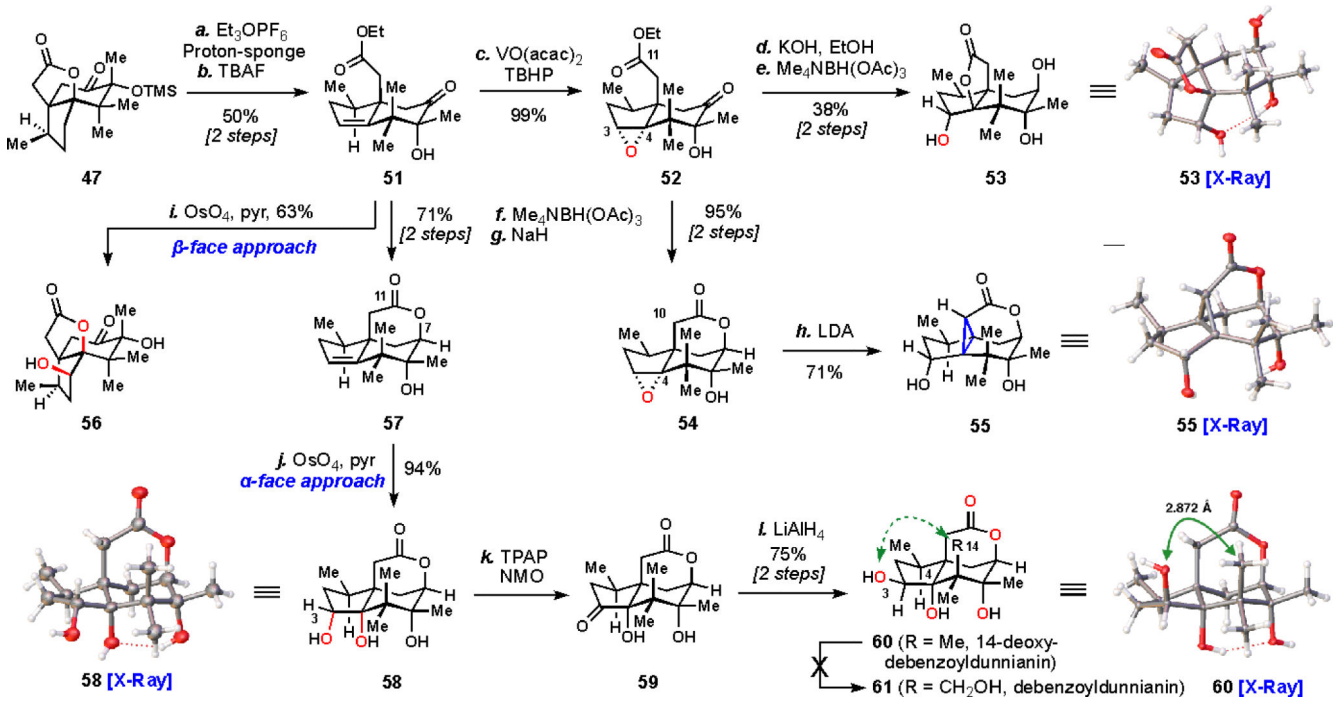

Scheme 2.

Synthesis of 14-Deoxydebenzoyldunnianin[a]

[a]Reagents and conditions: (a) Et_3OPF_6 (3.0 equiv), proton-sponge (3.0 equiv), DCM, 50 °C, 12 h; (b) TBAF (3.0 equiv), AcOH (3.0 equiv), THF, 12 h, 50% (*two steps*); (c) $VO(acac)_2$ (10 mol%), TBHP (*ca.* 5 M in decane, 2.5 equiv), PhH, 45 °C, 15 h, 99%; (d) KOH (10 wt% in H_2O, 10.0 equiv), EtOH, 3 h; (e) $Me_4NBH(OAc)_3$ (3.0 equiv), MeCN/THF/AcOH (4:1:1), –40 °C, 12 h, 38% (*two steps*); (f) $Me_4NBH(OAc)_3$, MeCN/AcOH (3:1), –40 °C, 12 h; (g) NaH (60 wt% in mineral oil, 3.0 equiv), THF, 1 h, 95% (*two steps from* 52) or 71% (*two steps from* 51); (h) LDA (3.0 equiv), THF, –78 °C, 1 h, 71%; (i) OsO_4 (1.2 equiv), pyridine, 12 h, *then add* $NaHSO_3$ (10.0 equiv), $MeOH/H_2O$ (3:1), 60 °C, 4 h, 63%; (j) OsO_4 (1.2 equiv), pyridine, 12 h, *then add* $NaHSO_3$ (10.0 equiv), $MeOH/H_2O$ (3:1), 60 °C, 4 h, 94%; (k) TPAP (10 mol%), NMO (2.1 equiv), DCM/MeCN (9:1), 18 h; (l) $LiAlH_4$ (2.0 M in THF, 3.1 equiv), THF, –78 °C, 2 h, 75% (*two steps*). Proton-sponge = 1,8-bis(dimethylamino)naphthalene, TBAF = tetra-*n*-butylammonium fluoride, TBHP = *tert*-butyl hydroperoxide, LDA = lithium diisopropylamide, TPAP = tetrapropylammonium perruthenate, NMO = *N*-methylmorpholine *N*-oxide.

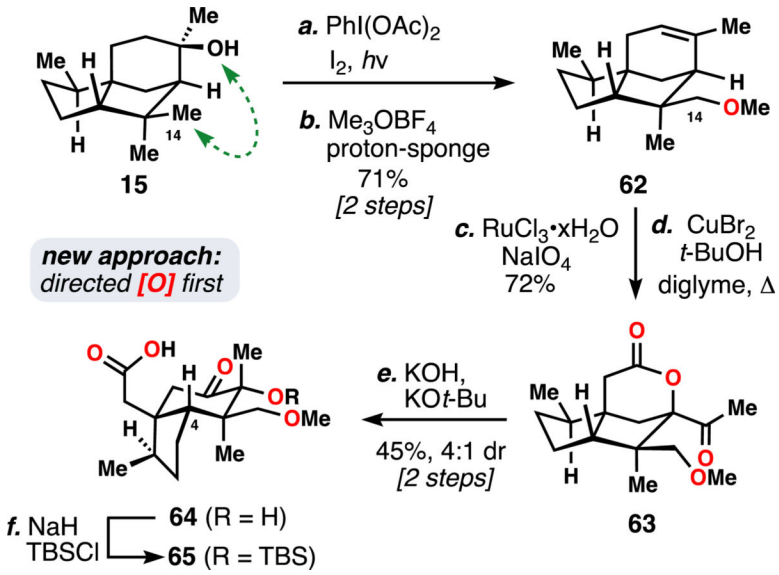

Scheme 3.

Successful Oxidation of C14[a]

[a]Reagents and conditions: (a) $PhI(OAc)_2$ (3.0 equiv), I_2 (1.0 equiv), cyclohexane, *hν* (visible), 1.5 h, 73%; (b) Me_3OBF_4 (1.5 equiv), proton sponge (1.5 equiv), DCM, 55 °C, 12 h, 97%; (c) $NaIO_4$ (5.0 equiv), $RuCl_3$•xH_2O (0.1 equiv), CCl_4:MeCN:H_2O (3:3:4), 1 h, 72%; d) $CuBr_2$ (3.0 equiv), *t*-BuOH (3.0 equiv), diglyme, 150 °C, 12 h; (e) KOH (1.0 equiv), KO*t*-Bu (3.0 equiv), DMSO, 14 h, 45% *(two steps)*, d.r. = 4:1; (f) NaH (5.0 equiv), TBSCl (4.0 equiv), THF, 65 °C, 8 h then add 3.0 M HCl (16 equiv), 65 °C, 16 h, 88%.

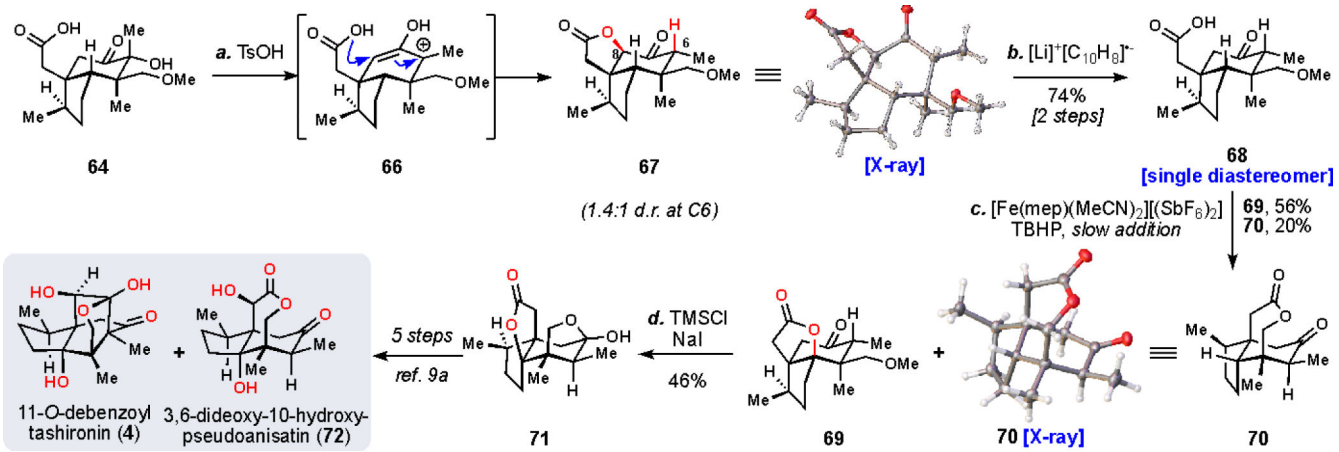

Scheme 4.

Formal Synthesis of 11-*O*-Debenzoyltashironin (4) and 3,6-Dideoxy-10-Hydroxypseudoanisatin (72)[a]

[a]Reagents and conditions: (a) TsOH•H_2O (1.5 equiv), DCE, 60 °C, 10 h, 1:1.4 d.r.; (b) lithium naphthalenide (3.0 equiv), THF, –78 °C, 10 min, 74% (two steps), >20:1 d.r.; (c) $[Fe(mep)(MeCN)_2][(SbF_6)_2]$ (50 mol%), TBHP (3.0 equiv), MeCN, 1 h, 56% 69, 20% 70; (d) TMSCl (10.0 equiv), NaI (5.0 equiv), MeCN, 80 °C, 45 min, 46%.

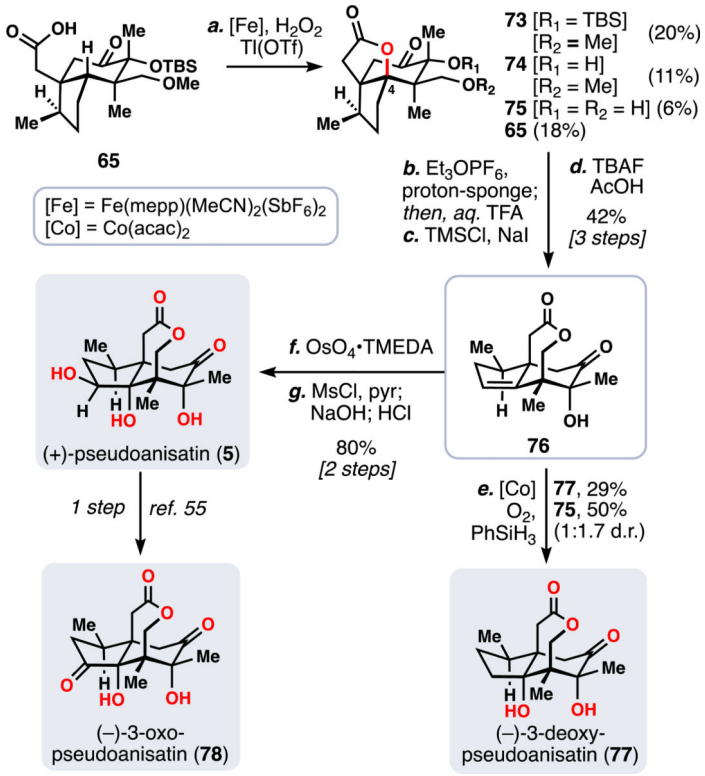

Scheme 5.

Synthesis of Pseudoanisatin (5), 3-Oxopseudo-anisatin (79), and 3-Deoxypseudoanisatin (78)

[a]Reagents and conditions: (a) TBHP (5.0 equiv), [Fe] (0.5 equiv), Tl(OTf) (0.5 equiv), MeCN, 1 h, 20% 74, 11% 75, 6% 76; (b) Et_3OPF_6 (3.0 equiv), proton sponge (3.0 equiv), DCE, 85 °C, 12 h *then add* TFA/H_2O (1:1), rt, 45 min, 66%; (c) TMSCl (10.0 equiv), NaI (5.0 equiv), MeCN, 80 °C, 12 h; (d) TBAF (5.0 equiv), AcOH (1.0 equiv), THF, 1 h, 64% *(two steps)*; (e) [Co] (0.1 equiv), $PhSiH_3$ (4.0 equiv), O_2 (1 atm), THF, 0 °C, 24 h; (f) OsO_4•TMEDA (1.5 equiv), DCM, −78 °C to rt, 2 h; (g) MsCl (10.0 equiv), pyr. (10.0 equiv), DCM, 12 h, then add *aq.* NaOH (2.0 M), 2 h, 80% (two steps).

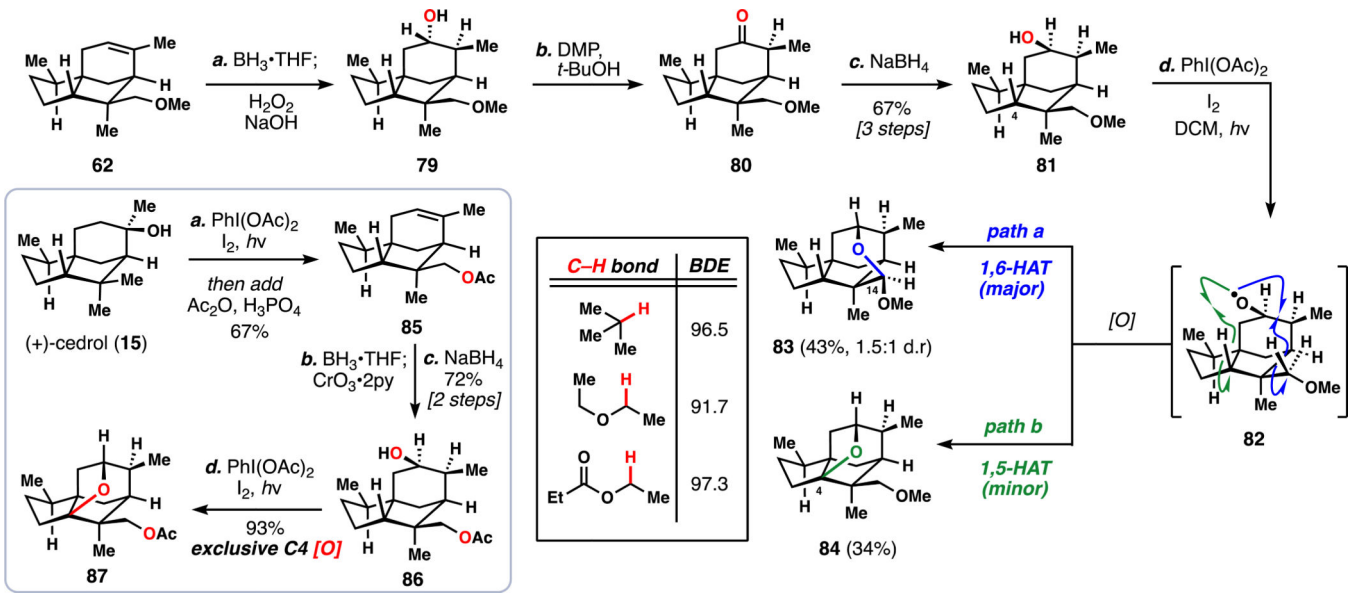

Scheme 6.

Studies on the Intramolecular C–H Abstraction of the C4 Methine Position[a]

[a]Reagents and conditions: (a) BH_3•THF (1.3 equiv), THF, 1.5 h *then* NaOH (3.6 equiv), H_2O_2 (5.0 equiv), 0 °C to rt, 10 min; (b) DMP (1.5 equiv), *t*-BuOH (3.0 equiv), DCM, rt, 30 min; (c) $NaBH_4$ (2.0 equiv), MeOH, rt, 30 min, 67% *(3 steps)*; Inset: (a) $PhI(OAc)_2$ (1.1 equiv), I_2 (0.4 equiv), cyclohexane, *hν* (visible), 1.5 h then Ac_2O (10.0 equiv), H_3PO_4 (2.0 equiv), 67%; (b) BH_3•THF (1.3 equiv), THF, 1.5 h *then* CrO_3•2pyr (25.0 equiv), DCM, 30 min; (c) $NaBH_4$ (1.5 equiv), MeOH, 30 min, 72% over two steps. (d) $PhI(OAc)_2$ (3.0 equiv), I_2 (1.0 equiv), DCM, *hν* (visible), 0 °C, 1.5 h, 93%

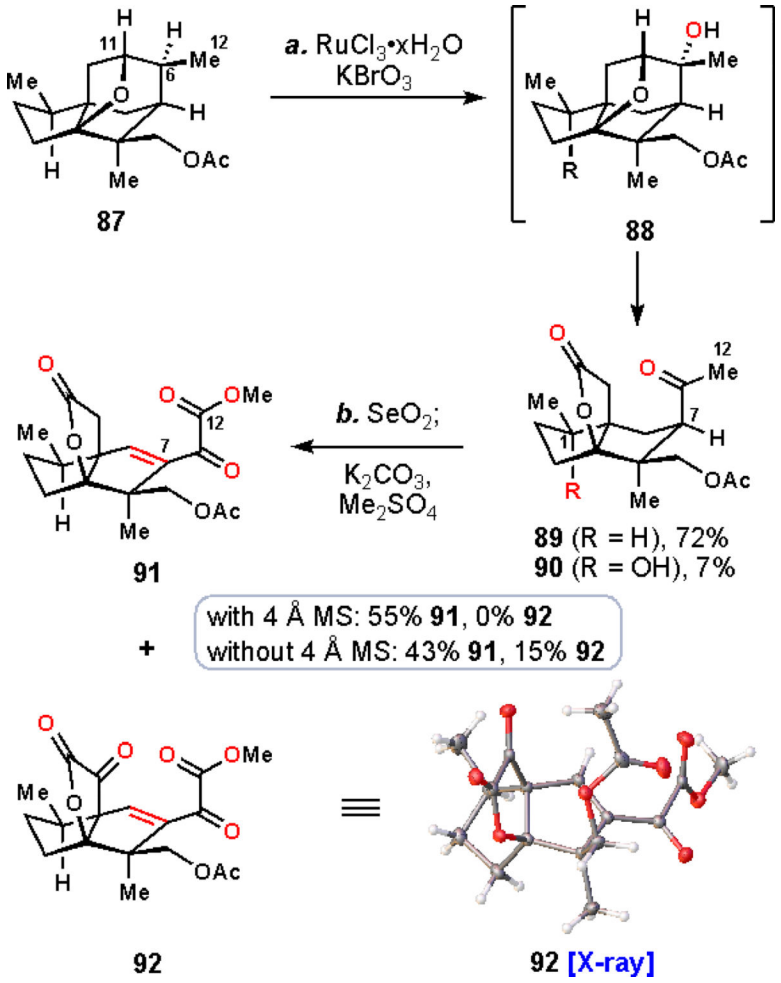

Scheme 7.

Ruthenium- and Selenium-Based Methods for the Near-Exhaustive Oxidation of 87[a]

[a]Reagents and conditions: (a) $RuCl_3$•xH_2O (3 × 3 mol%), $KBrO_3$ (2 × 5.0 equiv), CCl_4/MeCN/H_2O (2:2:3), 75 °C, 72 h, 72% 89, 7% 90; (b) SeO_2 (3.5 equiv), diglyme, 110 °C, 3 h, *then* K_2CO_3 (3.0 equiv), Me_2SO_4 (1.0 equiv), with 4 Å MS (1.0 mass equiv): 55% 91, without 4 Å MS, 43% 91, 15% 92.

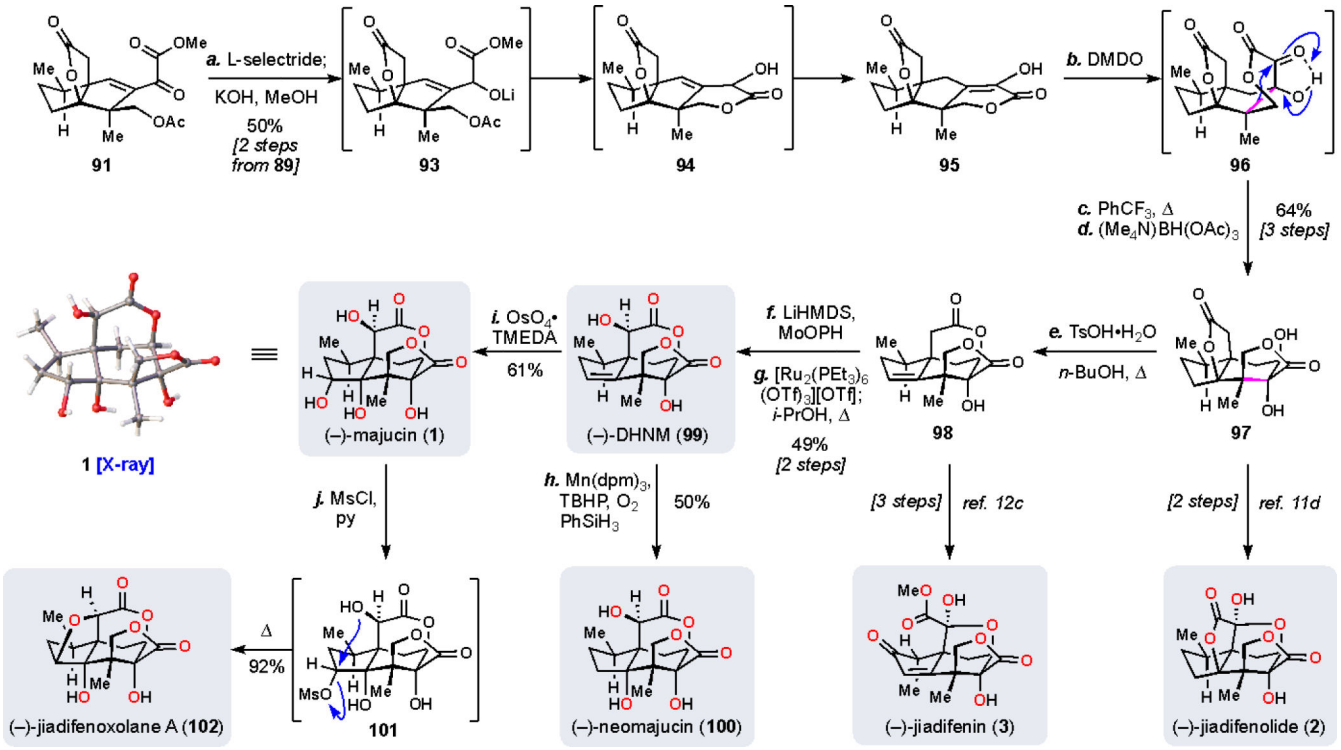

Scheme 8.

Synthesis of the Majucinoids[a]

[a]Reagents and conditions: (a) L-selectride (1.2 equiv), THF, −78 °C, 30 min *then* KOH (10.0 equiv), MeOH, 0 °C, 30 min, 50% *(two steps from 89)*; (b) DMDO (1.5 equiv), 12 h; (c) $PhCF_3$, 170 °C, 2 h; (d) $Me_4NBH(OAc)_3$ (7.0 equiv), MeCN/AcOH (3:1), −40 °C, 16 h, 64% *(three steps)*; (e) $TsOH•H_2O$ (2.2 equiv), *n*-BuOH, 150 °C, 26 h, 71%; (f) LHMDS (3.0 equiv), MoOPH (5.0 equiv), THF, −78 → 0 °C, 2.5 h, 65%; (g) $[Ru_2(PEt_3)_6(OTf)_3](OTf)$ (0.1 equiv), NMM (0.2 equiv), TFE/dioxane (1:1), 120 °C, 18 h *then* *i*-PrOH (3.0 equiv), 120 °C, 5 h, 75%; (h) $Mn(dpm)_3$ (0.2 equiv), TBHP (1.5 equiv), $PhSiH_3$ (2.0 equiv), O_2 (1 atm), DCM/*i*-PrOH (4:1), 0 °C, 20 h, 50%; (i) OsO_4•TMEDA (1.0 equiv), DCM, −78 → 0 °C, 2 h *then* $NaHSO_3$ (10.0 equiv), H_2O, 16 h, 61%; (j) MsCl (5.0 equiv), pyr. (10.0 equiv), DCE, rt →80 °C, 15 h, 92%. DMDO = dimethyldioxirane, LHMDS = lithium bis(trimethylsilyl)amide, MoOPH = oxodiperoxymolybdenum(pyridine) (hexamethylphosphoric triamide), dpm = dipivaloylmethane.

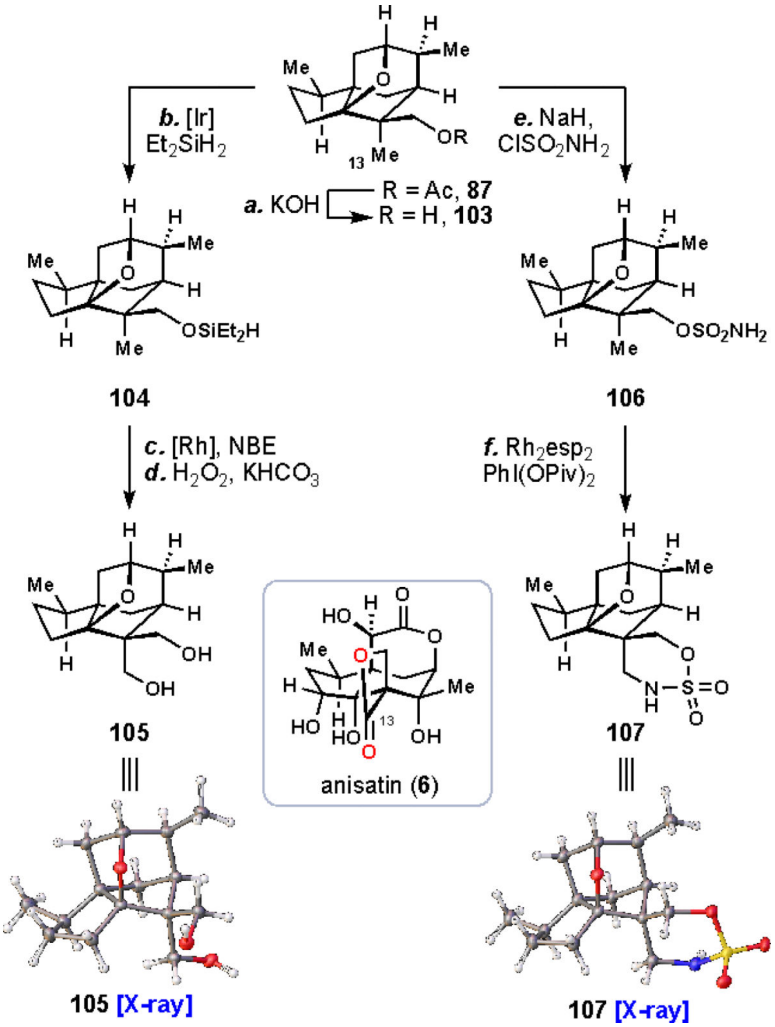

Scheme 9.

C–H Activation Studies of the Unactivated C13 Methyl Group[a]

[a]Reagents and conditions: (a) KOH (3.0 equiv), MeOH, 48 h, 91%; (b) $[Ir(COD)(OMe)]_2$ (0.5 mol %), Et_2SiH_2 (1.5 equiv), THF, 12 h; (c) $[Rh(COE)_2Cl]_2$ (2 mol %), (*S*)-DTBM-SegPhos (4 mol%), norbornene (1.2 equiv), THF, 100 °C, 12 h, 25% (*two steps*); (d) H_2O_2 (50 wt% in H_2O, 10.0 equiv), $KHCO_3$ (5.0 equiv), 50 °C, 36 h, 76%; (e) NaH (1.1 equiv), $ClSO_2NH_2$ (1.5 equiv), 0 → 23 °C, 4 h, 72%; (f) $Rh_2(esp)_2$ (3 mol%), $PhI(OPiv)_2$ (1.5 equiv), PhH, 16 h, 63%. esp = α,α,α′,α′-tetramethyl-1,3-benzenedipropionic acid.